This is to certify that the

dissertation entitled

Anionic Permeability of the

Liver ER Membrane

presented by

Ashutosh Tripathy

has been accepted towards fulfillment
of the requirements for

Ph.D. degree in Physiology

Major professor
H. Ti Tien, Ph.D.

Date Nov. 30, 1992

ANIONIC PERMEABILITY OF THE LIVER ER MEMBRANE

By

Ashutosh Tripathy

A THESIS

Submitted to
Michigan State University
in partial fulfillment of the requirements
for the degree of

DOCTOR OF PHILOSOPHY

Department of Physiology

1993

ABSTRACT

ANIONIC PERMEABILITY OF THE LIVER ER MEMBRANE

By

Ashutosh Tripathy

The ionic pathways present in the liver ER membrane are not known in detail. Studies using ER-derived vesicles have shown that they are permeable to Na^+, K^+, $choline^+$ and Cl^- but less permeable to Ca^{++} and Mg^{++}. Though highly permeable to K^+, the liver ER membrane has been postulated to lack an efficient ion conducting structure for K^+ like the K^+, Na^+ channel in the sarcoplasmic reticulum.

$InsP_3$, an intracellular second messenger can release Ca^{++} from an intracellular store of many types of cells and that store has been postulated to be the ER. An $InsP_3$-gated Ca^{++} channel has been shown to exist in canine cerebellar microsomes. But, the the identity of the store in liver tissue is unclear. Though the liver rough ER-derived vesicles have been shown to release Ca^{++} when challenged with $InsP_3$, the $InsP_3$- binding sites copurify not with the ER marker, rather with the plasma membrane marker.

The present study was undertaken with the aim to look at the anionic, Ca^{++} and K^+ permeability pathways present in the ER membrane.

Direct current-voltage recording is a straightforward approach to delineate the ionic pathways present in any membrane. But the membrane of an intracellular organelle like the ER is not accessible to direct cellular patch recording. So, we have fused the liver rough ER-derived vesicles with a planar BLM and have made current-voltage measurements across the reconstituted BLM. In our fusion protocols the vesicles could be readily fused with a BLM by swelling them osmotically in chloride containing solutions.

Using the above experimental approach, We have found that the liver rough ER-derived vesicles possess considerable anionic permeability. The permeability to halides and other anions follows the sequence : $SCN^- > I^- > Br^- > Cl^- >> gluconate^-$, suggesting that the chloride channels have low field-strength sites. It can be pharmacologically dissected to Zn^{++}-sensitive and DIDS-sensitive types. DIDS blocked the chloride permeability from the cytoplasmic side of the ER. No $InsP_3$-gated Ca^{++} channels, rynodine-sensitive Ca^{++} channels and K^+ channel were found in the liver rough ER membrane.

DEDICATION

To my parents, brothers and sisters
and my wife Moni and my son Arnav.

ACKNOWLEDGMENTS

I wish to express my sincere appreciation to my major adviser Dr. H. Ti Tien and to Drs. J. Krier, W. D. Atchison, R. A. Meyer, S. D. Mahanti, my guidance committee members for guidance and encouragement during the course of this study. I thank Dr. Dixon Woodbury of Wane State University for his help in making cups for the BLM studies.

I also wish to thank Dr. J. E. Chimoskey, Chairperson and Dr. C. C. Chou, Director of Graduate Studies, Department of Physiology for encouragement and support.

Special thanks go to my laboratory colleague, M. Zviman for help and cooperation and many interesting discussions on topics ranging from BLM to Bible.

And finally, mere words cannot express my gratitude to my wife Moni for her extreme patience, faith and encouragement and my three-year old son Arnav for enduring my constant absence. Arnav missed me a lot and I missed terribly a beautiful part of his growing up.

TABLE OF CONTENTS

LIST OF TABLES

LIST OF FIGURES

Figure Page

Figure Page

INTRODUCTION

All cells contain an endoplasmic reticulum (ER). Though highly convoluted, the ER membrane is thought to form a single continuous sheet, enclosing a single sac. The ER plays a central role in the biosynthesis of macromolecules used to construct other cellular organelles. Lipids, proteins and complex carbohydrates destined for transportation to the Golgi apparatus, to the plasma membrane, to the lysosome, or to the cell exterior are all synthesized in association with the ER. Two functionally distinct regions of the ER can be easily identified in some cells: the rough ER and the smooth ER. The rough ER is studded with ribosomes on the cytoplasmic side of the membrane. Numerous morphological investigations have demonstrated rough ER and smooth ER to be in direct physical continuity; rough ER is thought to give rise to smooth ER by a process of cisternal "budding." Physical disruption of the cells (homogenization) results in the conversion of both forms of ER into spherical vesicles which can be isolated as the microsomal fraction by differential centrifugation.

Several permeation systems for ions and small solutes are present within the reticulum structures of cells. Three transport proteins, T_1, T_2 and T_3 are required to enable glucose-6-phosphate, phosphate (and pyrophosphate), and glucose to respectively cross the ER membrane (1). Other biologically relevant solutes and ions that cross the ER membrane include D-glucose, L-glucose, L-leucine, choline$^+$, K^+, Na^+ and Cl^- (2). Meissner et al. (2) found that there are two types of liver microsomes (designated as types A and B) with differing permeabilities to glucose and other small molecules. About 70 percent of the

microsomes (type A) are permeable to D-glucose, L-glucose, 2-deoxy-D-glucose, D-mannose, D-mannitol, uridine, glycine, L-leucine, choline$^+$, TRIS$^+$, Rb^+, K^+, Na^+, and Cl^-. All of the above solutes, except Cl^-, pass with a comparatively slow rate in the remaining 30 percent type B vesicles. Type A and B vesicles are similar in that both are essentially impermeable to sucrose, yet permeable to Cl^-. By making membrane potential measurements with a fluorescent dye probe, Meissner et al. found that a significant fraction of ER vesicles were more permeable to TRIS$^+$ than to Ca^{++} or Mg^{++}. They also made another important observation that, despite their preferential permeability to K^+, a majority of liver microsomes lack an efficient ion-conducting structure for K^+, such as the K^+, Na^+ channel which renders above two-thirds of the SR vesicles highly permeable to K^+. Treatment with the anion transport inhibitor 4,4'-diisothiocyanostilbene-2,2'-disulfonic acid (DIDS) lowered the permeability of type A vesicles to several uncharged and negatively charged solutes, including D-glucose and gluconate$^-$. Based on their results, they suggested that a large fraction of liver microsomes is rendered permeable to various biologically relevant solutes and ions, perhaps through the presence of one or more channels with a maximum diameter of approximately 7-8 A° which select(s) against solutes on the basis of their size and charge.

The role of ER in sequestering Ca^{++} has been well recognized. Out of the two major intracellular organelles-i.e., the mitochondria and the ER, now there is general agreement, largely through the application of electron probe x-ray microanalysis to fast frozen tissue, that mitochondria contain little Ca^{++}, compatible with the regulation of mitochondrial enzymes but can sequester massive amounts, should the cytosolic Ca^{++} begin to rise and that, despite its relatively small Ca^{++}-binding capacity, the ER looks the stronger candidate for a high affinity physiologically relevant Ca^{++} store (3). A Ca^{++}-ATPase exists in

the ER membrane. The rat liver microsomal Ca^{++}-ATPase has been purified (4). Its molecular weight is 107 kDa and antiserum raised against the 100 kDa sarcoplasmic reticulum (SR) Ca^{++}-ATPase cross-reacted with it. A major Ca^{++}-binding protein, calreticulin (analogous to calsequestrin), has been shown to be present in the smooth muscle SR and liver ER (5). In this connection it should be borne in mind that SR, a specialized derivative of ER has long been known to be the intracellular Ca^{++} store in skeletal and cardiac muscle.

The rise to prominence of the ER has brought new ideas about Ca^{++} mobilization and, together with studies on the SR, a clear picture is beginning to emerge about the Ca^{++} sequestration and release processes and their control in these systems. A major step in this direction has been the discovery of inositol 1,4,5-trisphosphate ($InsP_3$) as an intracellular second messenger (6) and its role in releasing Ca^{++} from the ER of many types of cells (7). An inositol lipid located within the plasma membrane is the precursor used by the receptor mechanism to release $InsP_3$ to the cytosol, leaving 1,2-diacyl glycerol (DAG) within the plane of the membrane. Conceptually, this theory became very attractive, since, in one step, it provided a link between membrane receptors and release of Ca^{++} from a major intracellular store. Consistent with its role as a second messenger, the increase in the level of $InsP_3$ was found to precede the onset of Ca^{++}-dependent events in blowfly salivary gland (8) and in neutrophils (9). The transduction unit within the plasma membrane consists of three main components: 1) a receptor that detects the incoming signal; 2) a G protein that serves to couple the receptor to the third component; and 3) a phosphodiesterase responsible for cleaving the lipid precursor.

Ca^{++} is constantly cycling due to passive efflux and active influx across the ER membrane, and all the available evidence points to $InsP_3$ acting to stimulate the passive efflux component while having no effect on the pump.

$InsP_3$ had no effect on the Ca^{++} sequestering system of adipocytes (10) or parotid gland (11). Once Ca^{++} has been accumulated within the ER, inhibiting the pump by adding vanadate or by removing ATP results in a small release of Ca^{++}, which is enormously enhanced by addition of $InsP_3$ (12). The ability of $InsP_3$ to release Ca^{++} is independent of temperature (13,14,15), which suggests that $InsP_3$ acts by opening a channel. In order to release Ca^{++}, $InsP_3$ acts through a specific receptor, which may either be connected to or an integral part of the putative Ca^{++} channel.

Recently an $InsP_3$ receptor from cerebellum has been purified (16,17) and cloned (18). The reconstituted receptor was shown to support $InsP_3$-induced Ca^{++} fluxes from lipid vesicles (19,20) and to form Ca^{++}-permeable channels in planar lipid bilayers (21,22). These biochemical and molecular studies add support to the hypothesis that the receptor is an ion channel. The purified receptor has been shown to be a tetramer (23,24). The primary structure and biochemical properties of $InsP_3$ receptors from brain and smooth muscle have been reported to be very similar (25). It has been suggested that $InsP_3$-induced Ca^{++} release is highly cooperative (26). In reconstitution experiments involving planar bilayers, the $InsP_3$-gated Ca^{++} channel from canine cerebellar microsomes showed conductances of 20, 40, 60, and 80 pS with 50 mM Ca^{++} as the current carrier (27). These four conductance steps may reflect the interaction among the four $InsP_3$ receptors thought to comprise the $InsP_3$-gated Ca^{++} channel in that tissue. However, examination of the $InsP_3$ dependence of channel openings and Ca^{++} release from vesicles yielded a Hill coefficient of 1-1.3. So, it probably takes only one $InsP_3$ molecule to open the channel.

Though the $InsP_3$ receptor from cerebellum has been purified and functionally reconstituted, the relationship between this protein and the high-

affinity $InsP_3$ binding sites of peripheral tissues has been unclear. By comparing the $InsP_3$ binding sites of liver and cerebellum by measuring inhibition of specific $Ins^{32}P_3$ binding by various ligands under equilibrium conditions, it has been shown that the high affinity $InsP_3$ binding site of hepatocytes is likely to be the receptor that mediates Ca^{++} mobilization and that this receptor is at present indistinguishable from that in cerebellum (28). In their work with rough ER vesicles from liver, Muallem et al. had shown that $InsP_3$ can release Ca^{++} from these vesicles and that ATP-dependent Ca^{++} transport into the rough ER depends on the presence of tetra-ethylammonium-sensitive cation conductance and a furosemide-inhibited cation/Cl^- cotransport pathway and that $InsP_3$-induced Ca^{++} release requires K^+ to function as a counter ion (29).

However, in another study (30) comparing the distribution of $InsP_3$ binding sites and of the $InsP_3$-sensitive Ca^{++} pool and of other markers in various subcellular fractions, it has been shown that the $InsP_3$-binding vesicles appear to be completely distinct from the ER-derived microsomes. The $InsP_3$ binding sites were enriched in the same fraction which were enriched in alkaline phosphodiesterase I activity and that there is possible linkage between Ca^{++}-storing $InsP_3$-sensitive organelle and the plasma membrane through the actin microfilaments. In yet another study (31), a new name "calcisome" has been proposed for the $InsP_3$-sensitive Ca^{++} store in nonmuscle cells and the new organelles appear to be peculiar, heretofore unrecognized structures distributed throughout the cytoplasm.

In the SR, which is a specialized version of ER, a ryanodine-sensitive Ca^{++}-gated Ca^{++} channel has been shown to mediate Ca^{++} efflux (32,33). The channel has a large conductance of 170 pS in 50 mM barium. It is activated by adenine nucleotides and is blocked by ruthenium red (32,33). The ryanodine-sensitive channel has also been observed in brain microsomal preparations

(34,35,36). Using specific antibodies, both receptors have been found in Purkinje cells of cerebellum (37,38). For the $InsP_3$-gated Ca^{++} channel, the maximum probability of opening has been shown to occur at 0.2 μM free Ca^{++}, with sharp decreases on either side of the maximum, and the maximum activity for the ryanodine receptor/channel was maintained between 1 and 100 μM Ca^{++} (36). It has been proposed that the existence in the same cell of two channels with different responses to Ca^{++} and different ligand sensitivities provides a basis for complex patterns of intracellular Ca^{++} regulation (36). But in their studies on the characterization of high affinity ryanodine-binding sites of rat liver ER, Shoshan-Barmatz found that though the smooth microsomal membranes were enriched with ryanodine binding sites (39), the liver does not process mRNA for the skeletal muscle ryanodine receptor (40).

The following then emerge about the ionic pathways present on the liver rough ER membrane:

1. It is permeable to choline$^+$, K^+, Na^+, and Cl^- and relatively impermeable to Mg^{++} and Ca^{++}.
2. Though it has appreciable conductance to K^+, it has been postulated that no K^+ channel (such as the one present on muscle SR) exists for fast K^+ transport.
3. Though $InsP_3$ releases Ca^{++} in permeabilized hepatocytes and in isolated liver rough microsomes, the $InsP_3$ receptor in liver does not co-purify with the ER fraction; rather, it is enriched in the plasma membrane fraction.
4. The liver does not process mRNA for the ryanodine-sensitive receptor, and the ryanodine-sensitive receptor/channel is enriched in the smooth ER.

Direct current-voltage measurement is a straightforward approach to delineate the ionic pathways present on any membrane. Only a few studies have been done by directly fusing rough ER vesicles with a bilayer membrane

(BLM) and making current - voltage measurements. In one such study by Simon et al. (41), pancreatic rough ER vesicles were fused with a planar bilayer membrane (BLM). With 45 mM K^+ glutamate solution in both sides, some of their preparations yielded unitary conductances of 20, 55, 80, and 115 pS. In their more recent work (42), they found single channels of conductance 220 pS when puromycin was added at low concentrations (0.33 μM). They postulate that these high conductance channels are protein-conducting channels which are observed presumably as a result of puromycin-induced clearance of nascent protein chains from the lumen of the channel. These protein-permeable channels were hypothesized to exist in the rough ER membrane through which the NH_2-terminal extension of about 6-12 hydrophobic amino acids directs the growing polypeptide chain into the ER lumen (43). These channels closed when the salt concentration was raised to levels at which ribosomes detach from the membrane (150-400 mM) indicating that the attached ribosome keeps the channel in an open conformation.

We have fused liver rough ER vesicles with a pre-formed planar BLM and have made direct current - voltage measurements across the reconstituted BLM. We have exploited the high Cl^- permeability of the rough ER membranes to swell them osmotically in high concentrations (200-500 mM) of KCl (osmotic swelling in most cases is a prerequisite for fusion of vesicles with BLMs (44,45,46). Using this reconstituted system, we have looked at the following questions about the nature of the ionic pathways in the rough ER membrane.

Ca^{++} Conductance of the Rough ER Membrane

1. In the light of earlier contradictory observations that $InsP_3$ can release Ca^{++} from rough ER preparation, but that $InsP_3$ receptor does not co-purify

with the ER vesicular fraction, we have looked for an $InsP_3$-gated Ca^{++} channel in the rough ER membrane.

2. Since canine cerebellar microsomes contain both the $InsP_3$ receptor channel and the ryanodine-sensitive channel, we have looked for the ryanodine-sensitive Ca^{++} channel in the rough ER membrane.

Chloride Conductance of the Rough ER Membrane

In recent years, Cl^- channels have gained a level of respectability similar to that of the cationic channels. Since most Cl^- channels do not exhibit the profound voltage- and time-dependent behavior of cation selective channels, their contribution has often been dismissed as leak current in macroscopic electrophysiology. However, at the microscopic level, patch clamp experiments have begun to reveal the characteristics of single Cl^- channels in isolation. Cl^- currents have been reported in many different tissues including various nerve and epithelial preparations as well as different types of muscle. Many of the Cl^- channels are activated by various agonists like neurotransmitters, adenosine 3',5'-monophosphate (cAMP) and Ca^{++}. Cl^- channels activated by inhibitory neurotransmitters such as γ-aminobutyric acid (GABA) and glycine occur in the soma-dendritic membrane of majority of central nervous system neurons (47). The cystic fibrosis transmembrane conductance regulator (CFTR) Cl^- channel of airway epithelia is activated by cAMP-dependent phosphorylation (48,49). Ca^{++}-activated Cl^- currents have been described in detail in lachrymal gland cells (50), Xenopus oocytes (51) and smooth muscle cells (52,53). Like the Cl^- currents observed in smooth muscle, many, but not all, epithelial Cl^- channels are also activated by intracellular Ca^{++}. Recently, a cAMP-dependent Cl^- current in cardiac muscle has been reported (54) and the apparent cAMP dependence of the Cl^- current in cardiac muscle is similar to the Cl^-

conductances found in many types of secretory epithelium (55). Cl^- channels that are not directly gated by agonist molecules are known to be widely distributed in many cells (55). A large majority of anion-selective channels that have been characterized at the single-channel level display a halide permeability sequence that varies inversely with ionic radius: $I^- > Br^- > Cl^- > F^-$. A notable exception is the 20 pS Cl^- channel of *Torpedo californica* electroplax that also exhibits an unusual dimeric gating pattern (56). This *Torpedo* channel has been shown to mediate only $Cl^-$and Br^- current while I^- and F^- are impermeant. Aside from this exception, I^--permeable Cl^- channels can be divided into two classes according to their unitary conductance and voltage dependence of gating. Cl^- channels belonging to the first category of large conductance (BCl) anion channels exhibit an ohmic current-voltage relationship and have a unitary conductance of 200-500 pS in symmetrical (0.1-0.2 M) NaCl. Such BCl channels generally exhibit weaker ionic selectivity than small conductance (SCl) Cl^- channels in comparing Na^+ and K^+ permeability to Cl^- ($P_{Na^+,K^+}/P_{Cl^-} > 0.1$-0.2). They have a high open-state probability in a narrow voltage range near-0 mV with decreasing opening probability at large positive and negative voltages. Examples of BCl channels characterized in the plasma membrane of various cells include: rat Schwann cells, 450 pS (57); cultured rat skeletal muscle, 430 pS (58); rat aorta smooth muscle, 340 pS (52); rabbit urinary bladder, 360 pS (59); amphibian skeletal muscle (60); and amphibian kidney epithelia, 360 pS (61). Large conductance Cl^- channels have also been described in rabbit SR (62), frog SR (63) and mitochondrial outer membrane (64).

In contrast to the weak ionic selectivity and biphasic voltage dependence of BCl channels, the SCl channels display an outward rectifying, single-channel I-V behavior. Most of these channels also display a weak voltage dependence

of gating characterized by increased opening probability at positive voltage. Examples of SCI channels include Cl^- channels of apical membrane of rat colon epithelia, 40 pS (65); cultured human colon tumor cells, 50 pS (66); human airway epithelia, 30 pS (67); human lymphocytes, 39 pS (68); rat hippocampal neurons, 30 pS (69) and lobster neurons, 20 pS (70).

As has been mentioned earlier, the work by Meissner et al. (2) has demonstrated a large Cl^- permeability of the ER derived vesicles. In our attempt to fuse the microsomes with a BLM, we found that microsomes readily fuse with a BLM using 200-400 mM KCl as the osmoticant and the reconstituted BLM has appreciable Cl^- permeability. We decided to look at the nature of the Cl^- permeability of the rough ER vesicles, its ionic selectivity and pharmacology, both at the macroscopic and microscopic level and compare the above properties of the liver rough ER chloride channels with other chloride channels found in different systems.

EXPERIMENTAL DESIGN

The development of the patch clamp technique (71) has revolutionized the study of ionic channels, both in native and reconstituted membranes. Reconstitution of ion channels into planar lipid bilayers offers an added advantage in that it provides a practical approach to studying integral membrane proteins in a simple, chemically defined system in which fundamental mechanistic questions may be posed more easily than in the complicated native membrane (72). Moreover, the electrophysiological properties of intracellular organelle membranes, which are inaccessible to direct cellular recording, can be studied using electrophysiological techniques after reconstitution in a planar bilayer. In most applications, channels are transferred to the preformed planar BLM by fusing native membrane vesicles or liposomes containing purified channel proteins (44,45,73). There have also been attempts to make large vesicles from a population of smaller vesicles by repeatedly freezing and thawing the sample and then taking a patch out of the large vesicle (74). Another approach has been to make monolayers using the proteolipids extracted from native membranes and/or purified phospholipids and then to pick up two monolayers at the tip of a patch clamp micropipette to make a bilayer (34,75,76). The method has been appropriately called "double tip-dip" method. In all our experiments, we have designed and followed protocols to fuse the liver rough ER vesicles directly to a preformed planar BLM to delineate the Ca^{++} and Cl^{-} ionic pathways of the rough ER membrane.

Isolation of Rough ER Vesicles from Rat Liver

Isolation Procedure

Adult male Sprague-Dawley rats weighing 200-250 grams were used. The animals were fasted for 20 hr before sacrifice. Rough ER vesicles were isolated according to Dallner's procedure (77), which is a modification of the original procedure of Rothschild (78). Minced livers were homogenized relatively gently in 0.44 M sucrose, 2 g/10 ml, in a Teflon-glass homogenizer (4 x 400 rpm). After the first centrifugation at 10,000 *g* for 20 min, the supernatant was diluted with 0.44 M sucrose to restore the original volume. Of this suspension, 8 ml was layered over 3 ml of 1.31 M sucrose and centrifuged at 105,000 *g* for 7 hr 40 min in a Sorvall ultracentrifuge. The upper 0.44 M sucrose phase is removed. The milky layer localized in the upper part of 1.3 M sucrose phase, which is in the process of sedimenting down is removed, recentrifuged at 105,000 *g* for 90 min after dilution with 0.25 M sucrose containing 0.15 M KCl. It contains the smooth microsomes. The 1.3 M sucrose layer is removed and discarded, but the fluffy layer just above the pellet is left behind and is rehomogenized by hand together with the pellet, after the addition of a few drops of water, and centrifuged at 105,000 *g* for 90 min. It contains rough microsomes. All the solutions contained the protease inhibitors: 500 µg/ml EDTA, 0.5 µg/ml leupeptin, 0.7 µg/ml pepstatin, 100 µg/ml phenylmethylsulfonyl fluoride. After protein estimation, the smooth and rough microsomes are divided into small aliquots of 100 µl (10 mg/ml), quickly frozen in liquid N_2, and stored at -80 °C.

Protein Estimation

Protein was estimated using the Lowry procedure (79) using Bovine serum albumin as standard.

Assay for Marker Enzyme

NADPH-dependent cytochrome c reductase (marker enzyme for ER) activity was determined by colorimetric measurement of cytochrome c reduction in the presence of sodium azide and NADPH, utilizing the procedure of Fleischer and Fleischer (80).

Planar Bilayer Setup

We have used two types of planar bilayer cells. In the first type a polytetrafluoroethylene (PTFE) film of 50 μm thickness, on which a hole (200-300 μm diameter) has been punched by a leveled and electrically sharpened hypodermic needle, is clamped between two communicating perspex chambers (volume of each is 2 cc). The second type consists of two chambers formed by a polystyrene cup (volume 2 cc) inserted into a doubly cut-away polyvinylchloride (PVC) block. Very clean circular holes can be made on a PTFE film as follows:

1. A hypodermic needle, (27 gauge) is leveled by rubbing on a fine silicon carbide coated paper.
2. Sharpening is conducted in 5 M HCl solution applying 1.5 V (with the positive pole connected to the needle) and by repeated immersion and removal of the needle tip.
3. The PTFE film is supported on a new Plexiglas plate. The needle is mounted on a syringe and is brought down on the PTFE film. The hole is cut by a single turn around the axis.

The quality of the hole is checked under a microscope, but the ultimate test is the ease of forming membranes and their resistance and stability. The films are washed in 5 M KOH; chromic acid; hot water; distilled water; chloroform-methanol, 2:1 (v/v) and n-hexane and then dried in air before use.

Clean circular holes of diameters ranging between 50-250 μm can be made on a polystyrene cup as follows:

1. First make a protrusion on the outside wall of the polystyrene cup (wall thickness _ 1 mm) by pressing a heated blunt needle (450 °C) against the inner wall and advancing it forward until a slight protrusion can be felt on the outside wall by touching.
2. Slice off from the protrusion with a sharp microtome blade until a circular hole of proper size (100-200 μm) is exposed.
3. Heat polish the hole to make it smooth.

Each cup is inspected under a microscope to ensure that the hole is free from dirt and that cracks have not formed along the edge of the hole. Minute stress cracks radiating outward from the hole cause the bilayer to be mechanically unstable. Cups showing such signs of wear and tear are discarded. The cup is soaked in 4 percent (v/v) Joy liquid detergent for 3-4 hrs.; washed under running tap water for 1/2 hr.; soaked in distilled water for 1/2 hr.; given a few more rinses in distilled water and finally dried in air.

Electrophysiological Setup for Measurement

Ag/AgCl electrodes encased in 0.2 M KCl, 2 percent agar-filled lengths of polyethylene tubing, are inserted into each chamber for the purpose of applying and recording voltage pulses.

Figure 1 is a schematic diagram of a data recording, storage, and acquisition system. The command voltage is applied to and current measured across a BLM by a Dagan 8800 total clamp system. The data are monitored on the scope and simultaneously fed to a pulse code modulator (Neurocorder DR 484) and stored on a VCR (Hitachi). The Dagan total clamp system also has a direct current readout monitor. The data from the VCR is acquired off-line using

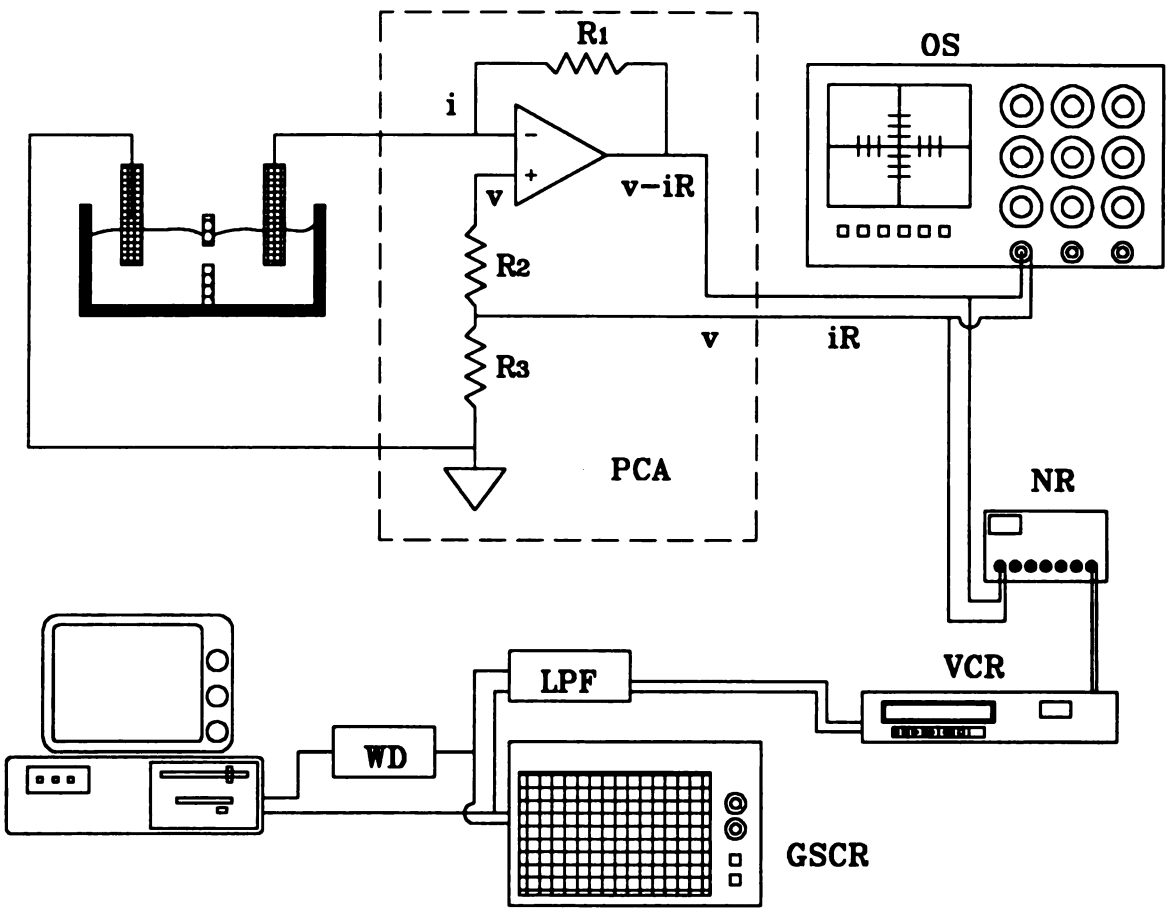

Figure 1. Diagrammatic representation of the BLM setup; R - Feedback resistor; v - Command voltage; i - Measured current; R_2, R_3 - Voltage dividing resistors for command voltage; OS - Oscilloscope; NR - Neurocorder; VCR - Video recorder; WD - Window discriminator; PCA - Patch clamp amplifier; LPF - 8 pole low pass Bessel filter; GSCR - Gould strip chart recorder.

a data acquisition board (Labmaster Scientific Solutions, Inc.), and a data acquisition program (PCLAMP, Version 5.0, Axon Instruments). During acquisition, amplified current from the VCR is filtered at 1 kHz through an 8-pole low pass Bessel filter (model 902, Frequency Devices). Output is also acquired in some cases, on a fast strip chart recorder (Gould 2400S).

Fusion of ER Vesicles with the BLM

The details of the mechanism of fusion are still unknown. However, empirical information acquired over the past 15 years has led to a set of conditions under which membrane vesicles or liposomes can be induced to fuse with planar BLMs.

Fusion of vesicles with a planar BLM has been shown to consist of two experimentally distinguishable steps (Figure 2). In the first, a very tight, close, and irreversible association between the vesicles and the planar membrane is formed. If the vesicular and/or planar membrane contains negatively charged lipids, the addition of millimolar levels of divalent cations promotes this step. In choosing divalent cation concentration, adsorption of vesicles to the BLM must be weighed against vesicle-vesicle aggregation. Divalent cations induce vesicle aggregation as well as planar membrane adhesion and aggregated vesicles fuse poorly. The association between vesicle and BLM in the "prefusion" step is not a point contact but rather an adhesion of a substantial fraction of the vesicle with the bilayer (81). Proteins such as fibronectin can also be used to induce adhesion (82). In the second step, the actual fusion of vesicular and planar membrane takes place. For the second fusion step to occur, in most cases it is necessary that an intravesicular hydrostatic pressure develop within those vesicles that are in the prefusion state. This pressure is routinely induced by osmotically swelling the vesicles and when lysis occurs in the region of contact

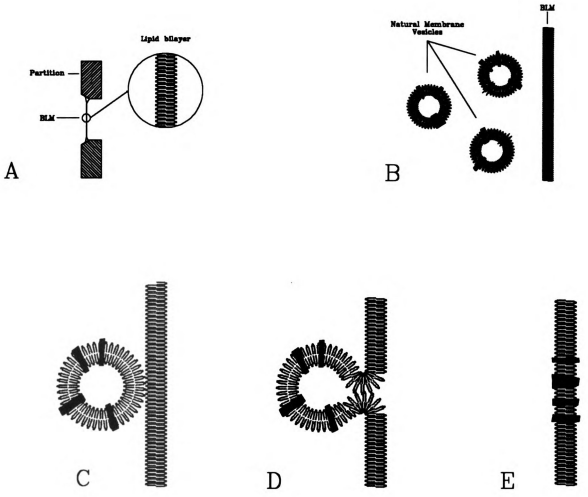

Figure 2. Schematic representation of fusion of vesicles with a planar BLM. A - scheme of a BLM. B - initial stage. C - prefusion state. D - osmotic swelling of the vesicle and fusion. E - final stage: reconstituted BLM.

between the vesicle and BLM, fusion occurs. The osmotic swelling of the vesicle is easily achieved by establishing an osmotic gradient across the planar BLM, *cis* side (the side to which vesicles are added) hyperosmotic with respect to the *trans* side. Water then flows from *trans* to *cis* and a fraction of it enters the vesicles in the prefusion step and causes them to swell. The osmotic gradient can be easily imposed across the BLM by simply adding an osmoticant to the side to which vesicles are added. Since the net role of the osmoticant is to cause swelling of the vesicles, it is necessary that the vesicle membrane be permeable to that osmoticant. Addition of vesicle-impermeant osmoticant will cause net shrinkage of the vesicles and will not promote fusion. The osmoticant also must not be too permeant through the BLM. If the osmoticant is too permeant through the BLM, it will be dissipated across the unstirred layers adjacent to the membrane and there will not be adequate net movement into the vesicle to cause swelling. Urea and glycerol fit into the above criteria and are good osmoticants. If the vesicular membrane has channels that allow salts to enter the vesicles, then permeant salts can be used to swell the vesicles osmotically. A 200-600 mOsm gradient across the BLM is generally sufficient to induce fusion (45,46,83).

Vesicles should be added to the *cis* side with continuous stirring. Stirring promotes adsorption of vesicles to BLMs (81). Vesicles can also be injected from a micropipette very near to the BLM. The probability of fusion is much higher using this method (84). When vesicles are added to the bulk aqueous phase, a final concentration of 1-10 µg/ml is generally sufficient.

For fusion to occur, the type of lipid used to make BLM is very important. Phospholipidethanolamine (PE) is a better phospholipid than phosphatidylcholine (PC) for promoting fusion. On the other hand, PC imparts stability to the BLM. A stable BLM is very desirable so that it can withstand the

various manipulations during experimentation. As mentioned earlier, sometimes it is necessary to incorporate a negatively charged lipid like phosphatidylserine (PS) in the BLM forming solution to promote the prefusion step. BLM forming solutions are normally made in n-decane with or without cholesterol. A lipid concentration of 15-50 mg/ml in n-decane is normally used as a BLM forming solution. When cholesterol is included in the BLM forming solution, the molar ratio between lipid and cholesterol is kept about 2:1 or 1:1. A less concentrated forming solution (15-20 mg/ml) has a greater molar ratio of the solvent n-decane compared to more concentrated solutions, and if BLMs are made using less concentrated solution, a greater amount of n-decane remains in the interior of the BLM. It has been shown that the fusion frequency is higher in these cases (73). It has been our consistent observation that BLMs made from a less concentrated solution are more prone to breakage during experimental manipulation of the BLM, especially while perfusing the *cis* and *trans* solutions.

An important step in vesicle-BLM fusion protocol is to stop further fusion after one or more vesicles have fused with the BLM. Fusion is stopped by abolishing the osmotic gradient by adding osmoticant to the *trans* compartment. Stopping the stirrer also halts further fusion. After fusion has been stopped, the *cis* solution which contains unfused vesicles can be perfused with fresh solutions.

A Typical Protocol for a BLM Reconstitution Experiment

BLM Forming Solution

A BLM forming solution is made by pipetting chloroform solutions of lipids into glass vials with a PTFE-lined stopper. The chloroform is evaporated with argon, the vial is evacuated for 20 min, and the lipids are resuspended in n-

decane (40 mg/ml). In all our experiments we have used a lipid mixture of PE:PS:PC in the ratio 5:3:2.

Preconditioning the Hole

Before painting a membrane across the hole, it is necessary to precondition the hole with a little BLM forming solution to achieve easy membrane formation. About 0.5 µl of the BLM forming solution is squirted into the hole, and a gentle stream of argon is directed toward the hole for 3-4 min. The *cis* and *trans* chambers are then immediately filled with aqueous solution.

Bilayer Formation, Fusion and Recording Buffers and Current – voltage Measurements

The BLM is made in a symmetrical bathing solution of 50 mM choline chloride plus 2 mM $CaCl_2$. We have limited the Ca^{++} concentration (it is needed to promote the prefusion step) to 2 mM, since it is known that ER vesicles aggregate in high concentrations of Ca^{++}. ER vesicles which normally need a final centrifugation of about 100,000 *g* to pellet them, can be pelleted at relatively low speed (27,000 *g*) by making microsomal aggregates in the presence of 8 mM Ca^{++} (85). To make the BLM, a little BLM forming solution is drawn into a micro-pipette tip and squirted out. The pipette tip is dipped in one of the aqueous chambers of the BLM setup and a bubble is blown by pressing the piston of the pippetor. The bubble is then smeared across the hole to make a BLM. The pipette tip is discarded after each use. Initially, a thick layer is formed at the orifice, and in reflected light interference colors can be seen. At this stage, the capacitance of the membrane is low. In a few min, the multilayer starts thinning to a bilayer state. The BLM looks grayish-dark in reflected light. Sometimes, the multilayer to bilayer transition can be initiated by applying an

electrical potential of negative 50-100 mV or by poking with one hair of a sable brush.

Membrane resistance is measured by applying a potential of ± 100 mV and measuring the resulting current. A typical orifice which has a diameter of 187 μm gives a current of ± 0.4 pA when ± 100 mV is imposed across the membrane. This calculates to a specific resistance of 0.68 x 10^8 Ω-cm which is in good agreement with literature values (86). The capacitance is measured by applying voltage pulses of 200 μV and noting the capacitative current transients. An integral of the current divided by the voltage gives the capacitance of the BLM:

$$C = \frac{\Delta Q}{\Delta V} = \frac{\int Idt}{\Delta V}$$

The capacitance value is about 0.7 μF/cm^2, again in good agreement with literature values (86).

Before every fusion protocol, the BLM was characterized optically and electrically (measuring capacitance and resistance of the BLM). In some of our initial experiments, to prove further that we had a BLM, we added a small quantity of gramicidin D (the bathing solution was 3 M KCl for gramicidin D experiments) and channel activity was recorded. Gramicidin channels are active only if it is a BLM (76).

The fusion protocol was initiated by raising the *cis* choline chloride concentration to 250 mM, by adding from a stock solution of 2.5 M choline chloride. The stirrer was switched on and after a few minutes, 15-20 μl (15-25 μg, about 10 μg/ml of *cis* buffer) of rough ER vesicles were added to the *cis* chamber. A membrane potential of -40 to -60 mV was applied to the *cis* side to aid fusion. Occurrence of fusion was shown by stepwise abrupt current changes. After fusion had occurred, the stirrer was switched off and to expose

the $InsP_3$-gated and ryanodine-sensitive Ca^{++} channels, the *cis* chamber was perfused with a solution of 60 mM piperazine-N,N'bis (2-ethanesulfonic acid) (PIPES) + 88 mM bistrispropane (BTP) (pH - 7.4). For recording $InsP_3$-gated Ca^{++} channels the cis solution also contained 1 mM EGTA + 0.5 mM $Ca(OH)_2$ (free Ca^{++} conc. 0.25 μM).and for recording rynodine-sensitive Ca^{++} channels the cis solution contained 0.1 mM EGTA + 0.1 mM $Ca(OH)_2$ (free Ca^{++} conc. 2.5 μM). The *trans* side was perfused with a solution having composition: 60 mM PIPES + 55 mM $Ca(OH)_2$ (pH 7.4). During perfusion, the *cis* side was shorted to the *trans* (electrical ground) side.

Our success rate of perfusing both chambers and leaving the BLM intact was very low. So, we modified the above procedure and designed a protocol, so that we have to perfuse only the *cis* side of the BLM.

In our modified procedure, BLMs were made in a symmetrical solution having the composition: 5 mM N-[2-hydroxyethyl] piperazine N'-[2-ethane sulfonic acid] (HEPES) + 1.3 mM $Ca(OH)_2$ (pH -7.4) or 2.2 mM PIPES + 2 mM $Ca(OH)_2$ (pH -7.4). After BLM was characterized by resistance and capacitance measurement, 100-200 μl of 4 M KCl (or potassium acetate) was added to the *cis* side making the final *cis* KCl (or potassium acetate) concentration 200-400 mM. After fusion, the *cis* solution was perfused with the solution having 0.25 μM free Ca^{++} (for $InsP_3$-gated channels) or 2.5 μM free Ca^{++} (for rynodine-sensitive Ca^{++} channels) The *trans* Ca^{++} concentration now can be raised to the desired level by adding from a concentrated stock solution of PIPES + $Ca(OH)_2$ or HEPES + $Ca(OH)_2$.

The above two-step protocol was necessary to fuse the ER vesicle and look for any Ca^{++} channels.

For measurement of Cl^- current, the bathing solution had the composition 5 mM HEPES + 1.3 mM $Ca(OH)_2$ + 2 mM KCl (pH -7.4). After BLM formation

and characterization, the *cis* KCl concentration was raised to 200-400 mM by adding 100-200 µl from a stock solution of 4 M KCl. After fusion of one or more vesicles, further fusion is prevented by stopping the stirrer and abolishing the osmotic gradient by adding sucrose solution to the *trans* side. For current measurement under bi-ionic conditions, the other salt solution is added to the *trans* side. In some of our experiments, we have perfused the *cis* side after fusion and have increased the *cis* and *trans* KCl concentration symmetrically by adding from a stock solution of 4 M KCl.

In another set of experiments to study the Cl^- channel, we used symmetrical 10 mM TRIS-HCl as the bathing solution. Fusion of rough ER vesicles with the BLM was achieved by adding 100-200 µl of 4 M KCl solution to the *cis* side (final KCl concentration: 200-400 mM). After one or a few vesicles had fused, the *cis* side was perfused with 10 mM TRIS-HCl to stop further fusion. Then KCl was added from a 4 M stock solution to the *cis* and *trans* side to symmetrically raise KCl concentration from 0 to 500 mM in steps of 50 or 100 mM. In each case, the conductance of the channel was measured by making current - voltage measurements.

The selectivity sequence of the various anions were found by measuring the reversal potential under bi-ionic conditions and applying the Goldman-Hodgkin-Katz (GHK) equation (87).

Stock solutions of various pharmacological agents were made as follows:

1. A 20 mM DIDS stock solution was made in 100 mM $KHCO_3$ solution (pH 8.0). 1 mM and 2 mM stocks were made by diluting a small quantity of 20 mM stock with appropriate amount of buffer.
2. Stock solutions of 60 mM and 75 mM and 300 mM $ZnCl_2$ were made in distilled water (acidified with a few drops of HCl).

3. A 0.5 M stock solution of tetraethylammoniumbromide (TEABr) was made in aqueous buffer.

All the fusion and recording buffer solutions for BLM reconstitution experiments were filtered using disposable filter units (pore size 0.22 μm).

RESULTS

Assay of Marker Enzyme for ER

NADPH-dependent cytochrome c reductase activity was determined by colorimetric measurement of cytochrome c reduction in the presence of sodium azide and NADPH. Figure 3A shows the optical density of the incubated mixture at 25 °C, measured at 550 nm as a function of time. The mixture contained the smooth ER vesicles. Taking the extinction coefficient for cytochrome c as 18.5 mM^{-1} cm^{-1} and using the initial linear portion of the curve, we can calculate the cytochrome c reductase activity in the smooth microsomes to be 54 nanomoles/min/mg protein.

Figure 3B shows the cytochrome c reductase activity of the rough ER vesicles at 25 °C and from the linear portion of the curve, we can calculate a specific activity for cytochrome c reductase in the rough ER membrane as 16.2 nanomoles/min/mg protein.

Smooth to rough ratio of NADPH-dependent cytochrome c reductase activity is calculated to be 3.3 and is close to the value 3.5 reported for the above enzyme in rabbit liver (88). The specific activity of the enzyme in rat liver microsomes as reported in literature (89), is 90 nanomoles/min/mg at 30 °C and assuming a Q_{10} of 2.5 for this enzyme, our values are within reasonable limits.

Characterization of a BLM

A BLM forming solution of PE:PS:PC in the ratio of 5:3:2 in n-decane (40 mg/ml) is used for making the BLM. The BLM is made in symmetrical 50 mM choline chloride solution. It is monitored optically as well as by measurement of electrical parameters like resistance and capacitance. Figure 4 depicts a typical

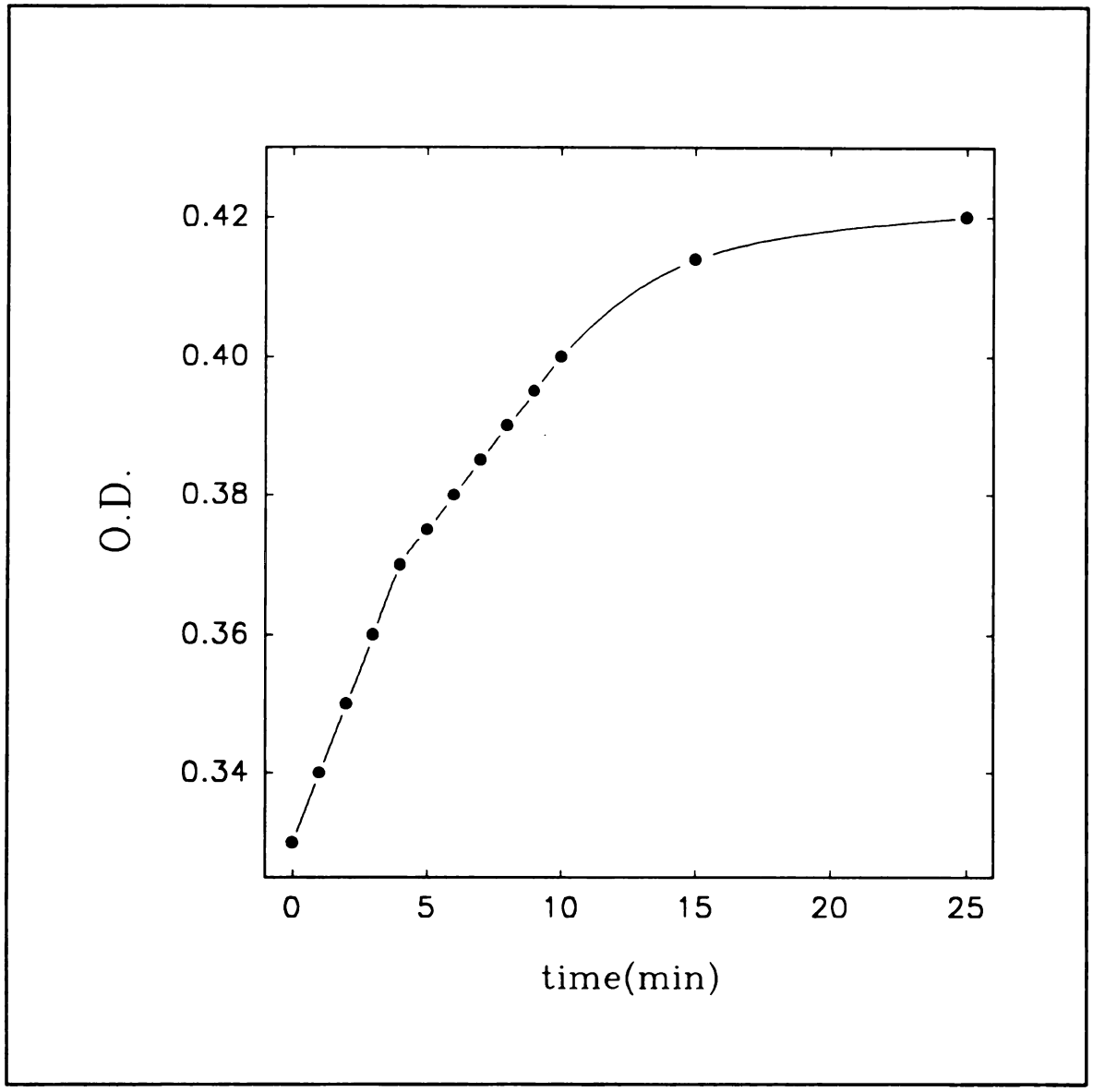

Figure 3A. Time course of reduction of cyt-c by liver smooth ER vesicular NADPH-dependent cyt-c reductase. Protein concentration is 11.6 µg/ml.

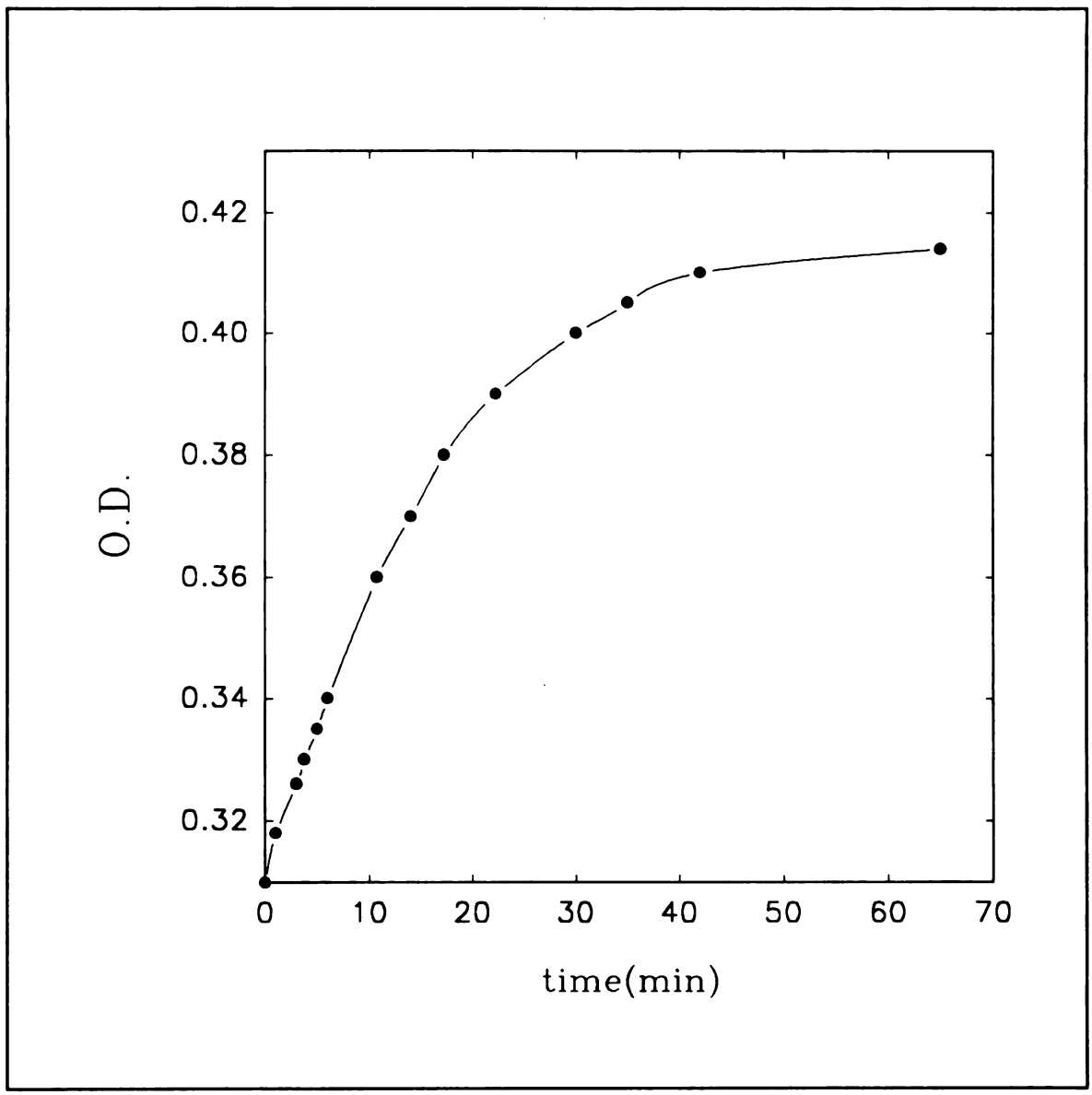

Figure 3B. Time course of reduction of cyt-c by liver rough ER vesicular NADPH-dependent cyt-c reductase. Protein concentration is 11.6 µg/ml.

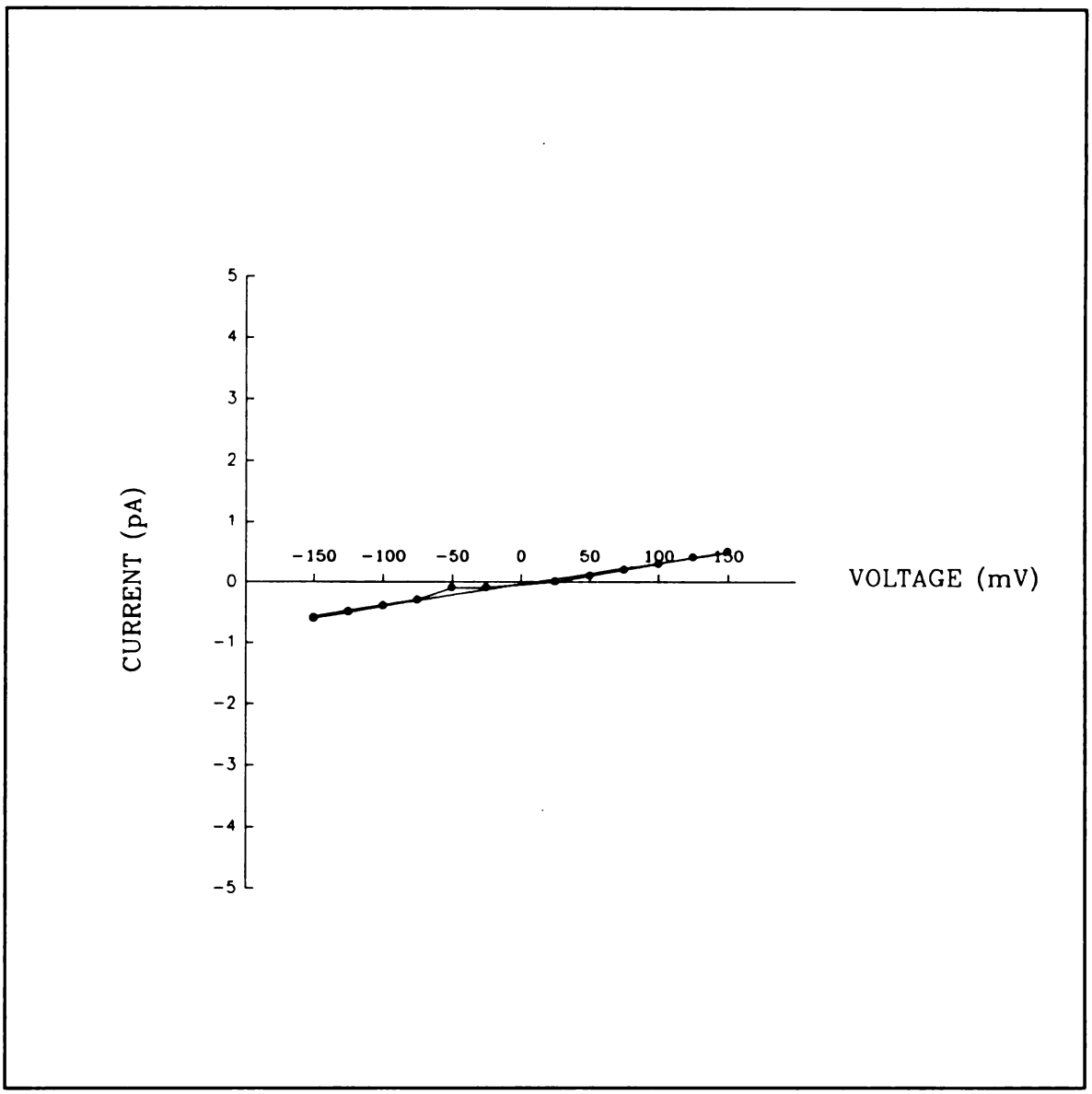

Figure 4. I-V curve of an unmodified BLM. The BLM was made in symmetrical 50 mM choline chloride solution. DC voltage steps were applied and current was measured in each case.

current-voltage relationship of an unmodified BLM. The conductance calculated from the slope of the curve is about 3-5 pS. A typical BLM of 200 μm diameter has a resistance of about 250 GΩ and one can calculate a specific resistance of $2.5x10^7$ Ω-cm. The capacitance of the BLM was measured by applying a voltage pulse of 200 μV and measuring the integral of the capacitative current transient. The resultant ΔQ divided by ΔV gives the capacitance of the membrane. Most of our BLMs had a capacitance between 0.55-0.7 $\mu F/cm^2$.

To prove further that we have a BLM, we incorporated gramicidin channels into a BLM. An example of one such gramicidin channel opening and closing transitions, is shown in Figure 5. Such current transitions were obtained at 250 mV in 3 M symmetrical KCl solution. From the current amplitudes, one can calculate a conductance of 25 pS which is very close to the value of found in literature (87).

Incorporation of ER Vesicles in a BLM in Asymmetric Choline Chloride Solution

The protocol for fusion is given schematically in Figure 6A. After BLM formation, the *cis* choline chloride concentration is raised to 250 mM to provide the osmotic gradient. Fusion usually occurs in 1-2 min. Typical fusion events are as shown in Figure 7A, in which the Y-axis denotes the current across the BLM and the X-axis time. The holding voltage is zero mV. At the beginning of the record, the current is almost zero and it changes in stepwise fashion in the outward direction when a vesicle fuses with the BLM. We can see two outward current jumps in Figure 7A, which suggests that two vesicles have fused with the BLM. Notice that even if the holding voltage is zero mV across the BLM, there is current flow because of the ionic gradient across the BLM. Since there is a choline chloride gradient from *cis* to *trans* and the current is outward, we can

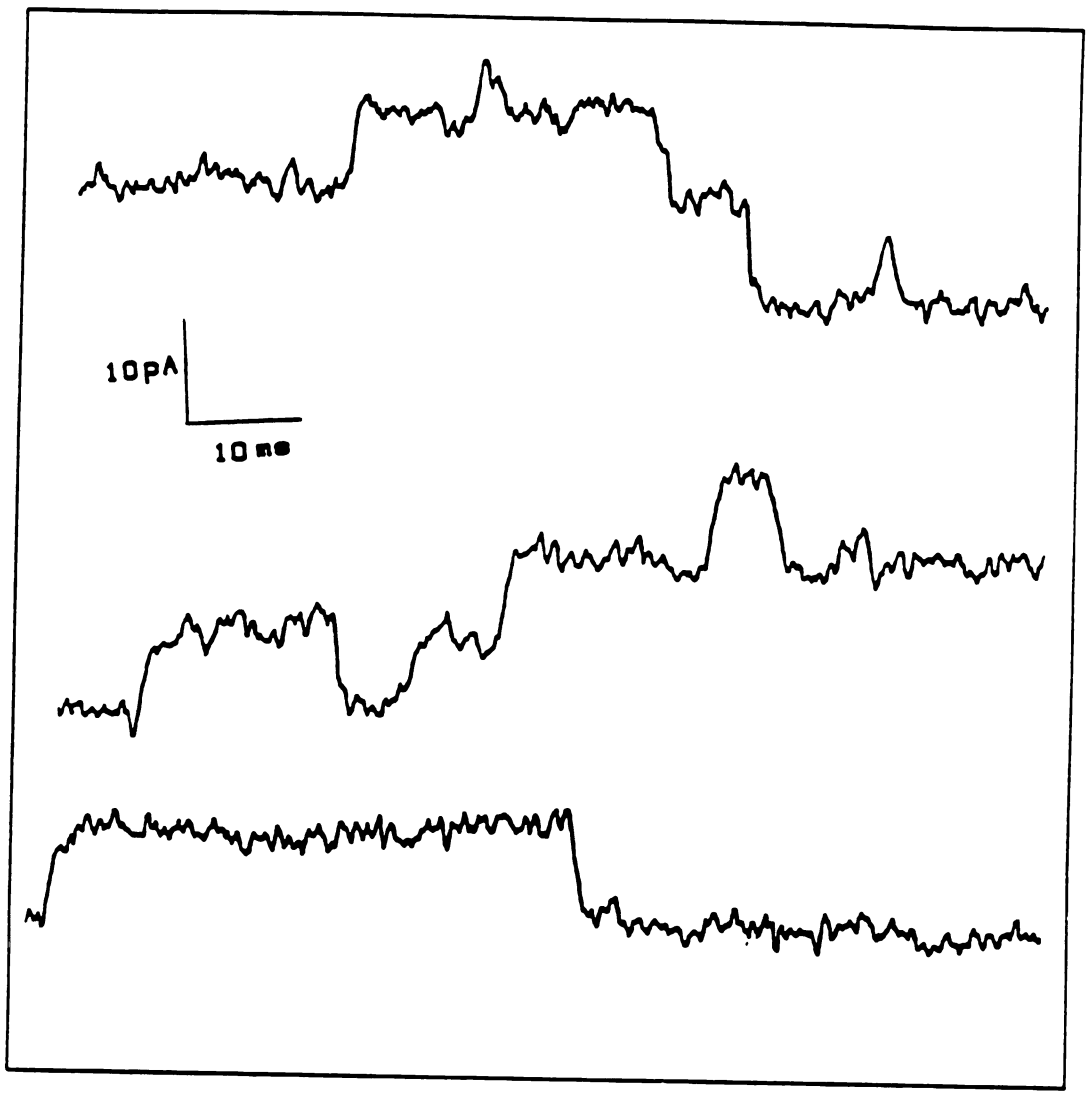

Figure 5. Gramicidin channels incorporated in BLM. The bathing solution is symmetrical 3 M KCl.

A.

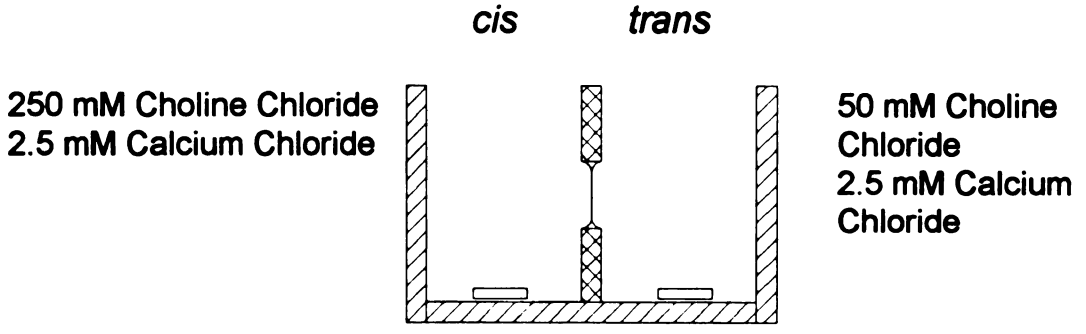

Perfuse *cis* and *trans* chambers

B.

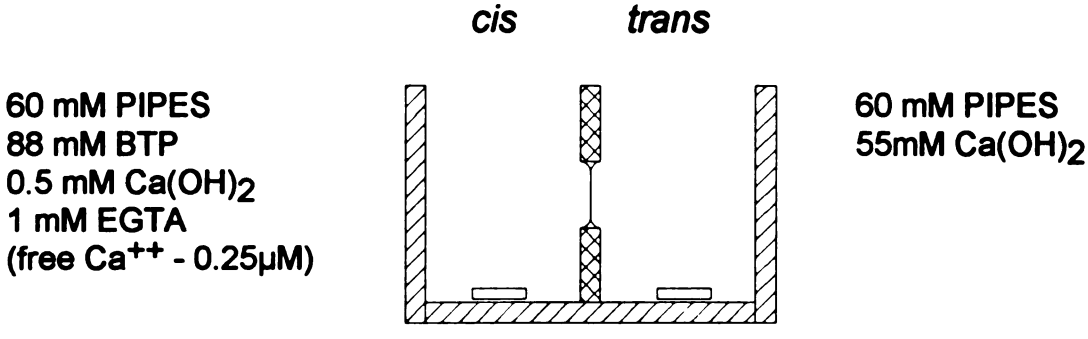

Figure 6 Schemes of the protocols for fusion of ER vesicles with a BLM (A) and recording of calcium channels (B).

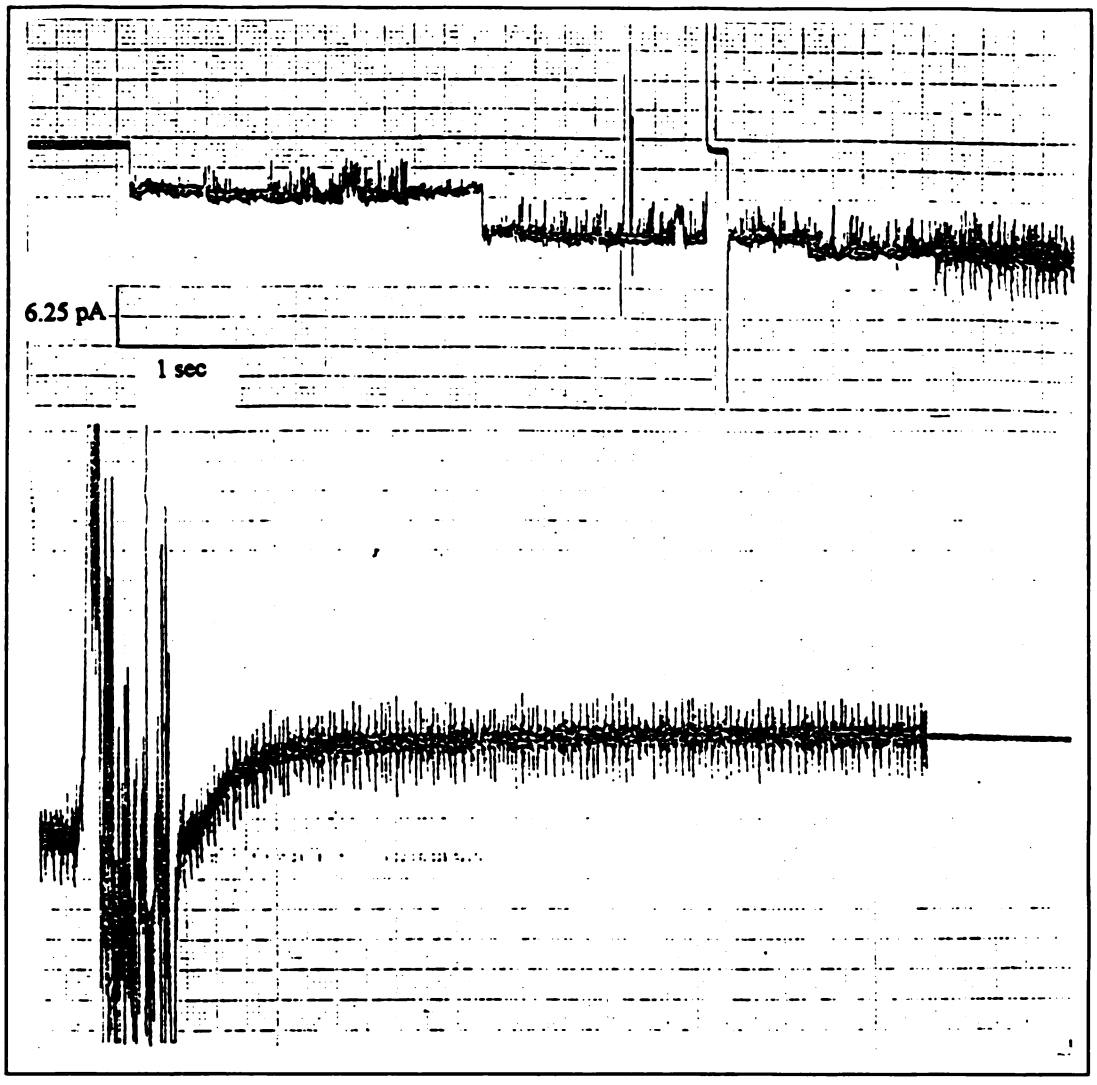

Figure 7. Typical observations of current jumps when ER vesicles fuse with a BLM (A). The bathing solution is symmetrical 50 mM choline chloride. Fusion is initiated by raising the *cis* choline chloride concentration to 250 mM and adding ER vesicles to the *cis* side (10 µg/ml). The current returns to zero when the *trans* choline chloride concentration is raised to 250 mM (B).

conclude that the majority of the charge carriers are Cl^- ions. When the choline chloride gradient is abolished by raising the *trans* choline chloride concentration to 250 mM, the current goes back to zero. This is depicted in Figure 7B.

A typical current-voltage relationship of a BLM reconstituted with liver ER vesicles in asymmetric choline chloride solution (*cis*-250 mM, *trans* - 50 mM) is shown in Figure 8. The reversal potential is at 25 mV. If Cl^- ions are the only charge carriers from the Nernst equation (87), we can calculate a reversal potential of 41 mV. Since the observed potential is 25 mV, it suggests an appreciable choline permeability through the Cl^- channels and applying Goldman-Hodgkin-Katz equation (87), written for a bi-ionic situation, in which the only species are choline and Cl^-:

$$V_{rev} = \frac{RT}{F} \ln \frac{P_{choline}[choline]_t + P_{Cl}[Cl]_c}{P_{choline}[choline]_c + P_{Cl}[Cl]_t}$$

where RT/F = 25.4 mV at 22 °C, the subscripts on the concentration terms refer to *cis* (c) and *trans* (t) and P_{Cl} and $P_{choline}$ are the respective permeabilities for Cl^- and choline ions. A quick calculation shows that $P_{Cl}/P_{choline}$ is about 5. Figure 9 depicts a series of current-voltage curves of a BLM reconstituted with liver ER vesicles in asymmetric choline chloride solution. Each symbol denotes a different membrane. After reconstitution, when the ionic gradient is abolished by raising the *trans* choline chloride concentration to 250 mM, the reversal potential becomes zero and this is shown in Figure 10.

Perfusion of the *cis* and *trans* Chambers with Only Ca^{++}-Containing Solutions

The protocol for this is shown schematically in Figure 6B. Briefly, after a fusion has occurred, the *trans* side is perfused with a solution containing 60 mM PIPES + 55 mM $Ca(OH)_2$ (pH-7.4) and the *cis* side is perfused with a solution

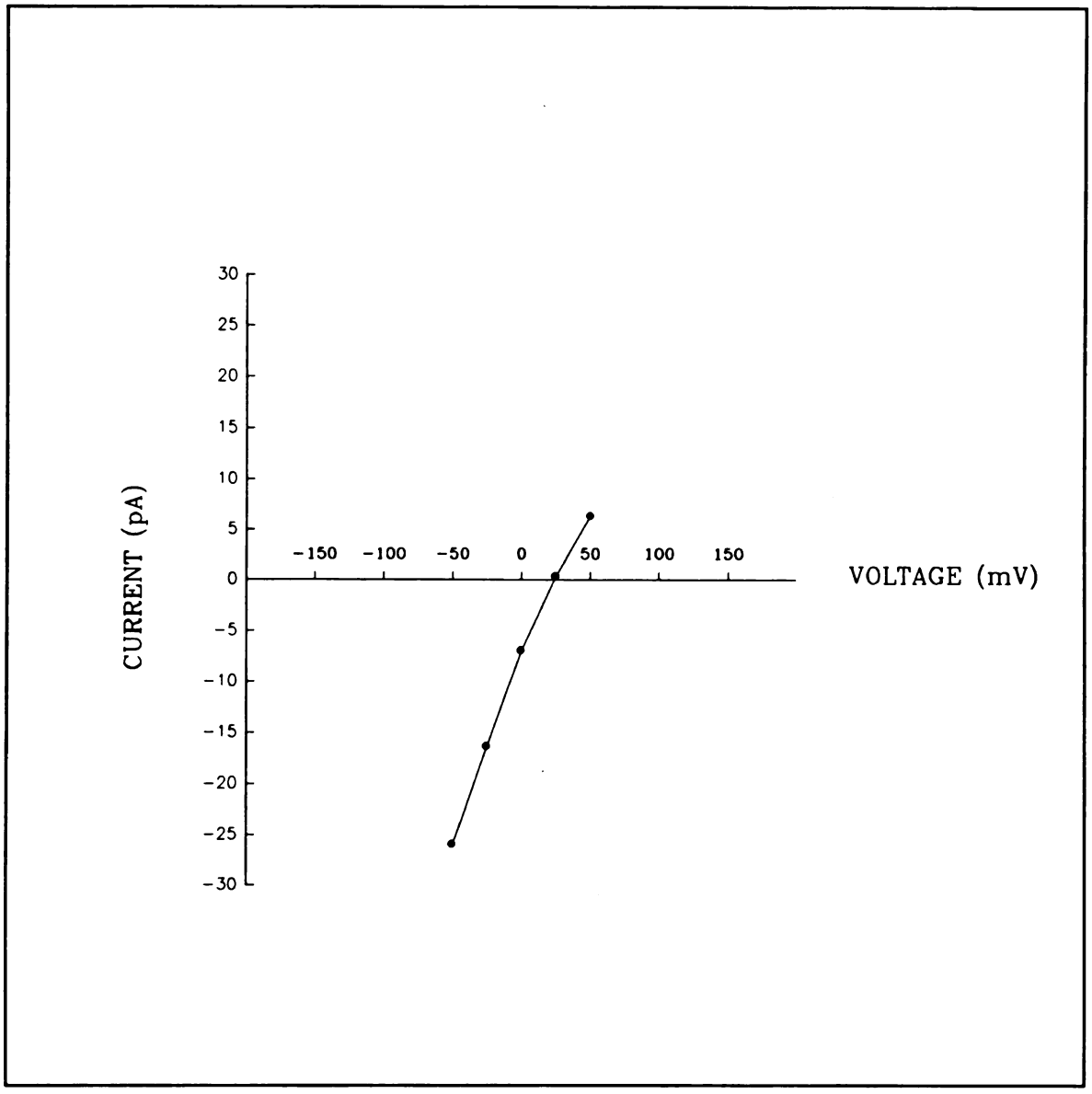

Figure 8. I-V relationship of a BLM reconstituted with liver ER vesicles. Vesicles were fused with a BLM in asymmetrical choline chloride solution (*cis* - 250 mM, *trans* - 50mM). The solution also contained 2.5 mM calcium chloride. After fusion, dc voltage steps were applied and current measured in each case.

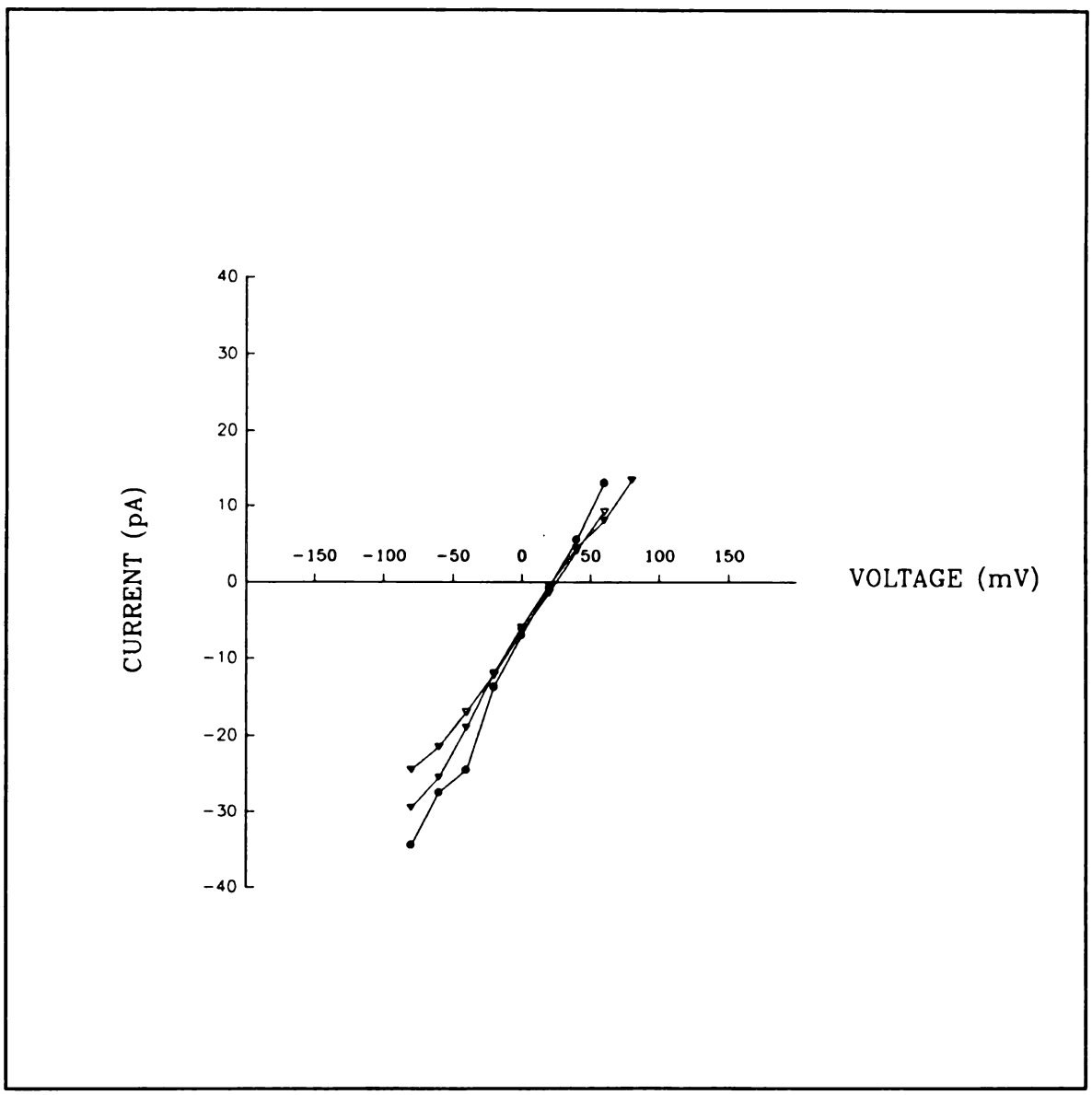

Figure 9. I-V curves of BLMs reconstituted with liver ER vesicles. Vesicles were made to fuse with a BLM in asymmetrical choline chloride solution (*cis* - 250 mM, *trans* - 50mM). The solution also contained 2.5 mM calcium chloride. After fusion, dc voltage steps were applied and current measured in each case. Each symbol represents a different membrane.

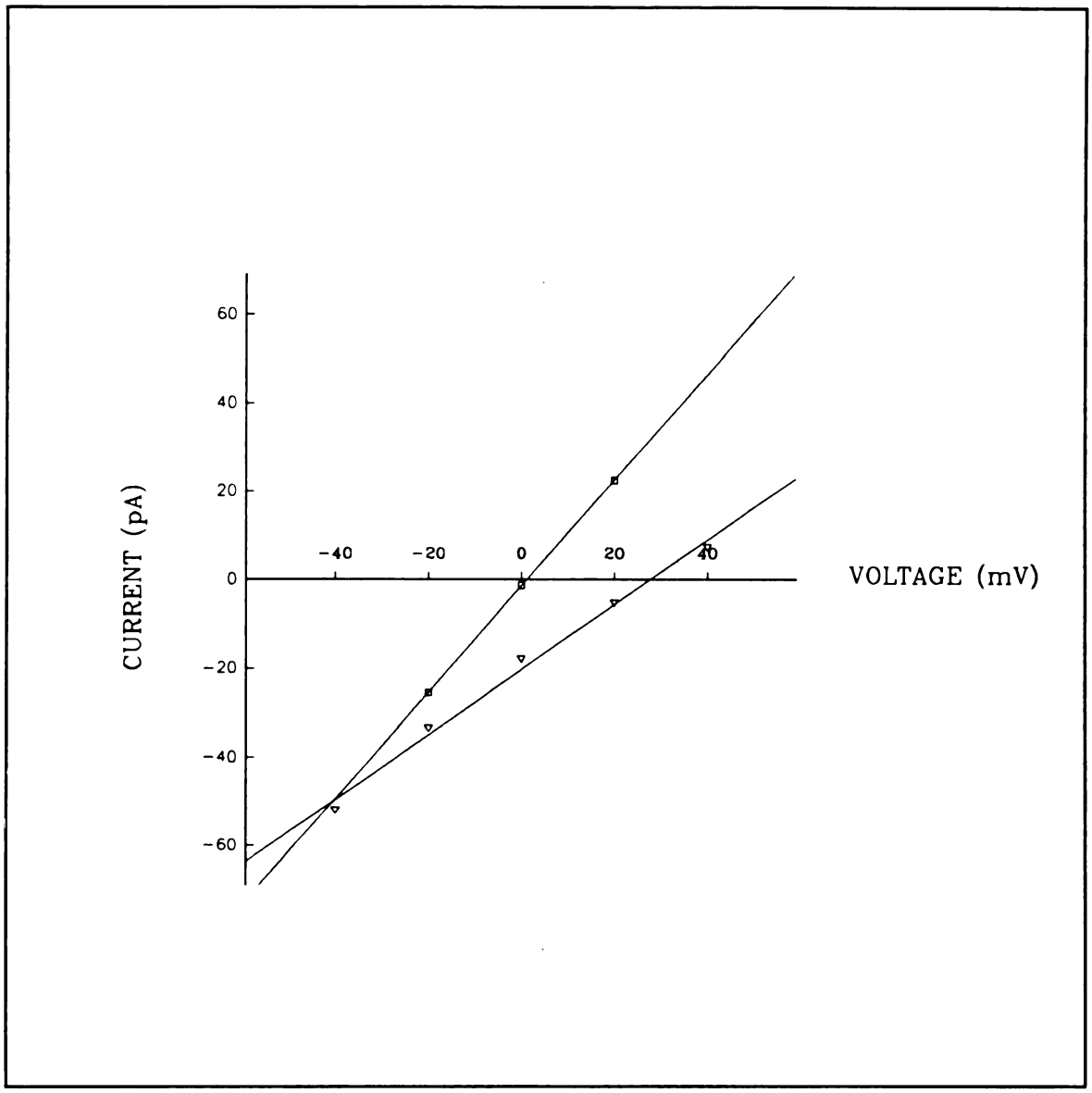

Figure 10. I-V curve of a BLM reconstituted with liver ER vesicles. Fusion was induced in asymmetrical choline chloride (*cis* - 250 mM, *trans* 50 mM) solution. After fusion, dc voltage steps were applied and current measured. I-V curve (∇ - ∇) in asymmetrical choline chloride (*cis* - 250 mM, *trans* 50 mM) solutions and (□ - □) in symmetrical choline chloride (*cis*, *trans* - 250mM).

containing 60 mM PIPES + 88 mM BTP + 0.5 mM $Ca(OH)_2$ + 1 mM EGTA (pH-7.4). A free Ca^{++} concentration in this solution was calculated to be 0.25 μM using the computer program of Fabiato (90) (for studying rynodine-sensitive Ca^{++}channels the cis solution contained 0.1 mM EGTA + 0.1 mM $Ca(OH)_2$, free Ca^{++} conc. 2.5 μM). During perfusion, the *cis* and *trans* chambers were short-circuted. Since our success rate of having intact BLMs after perfusing both sides was very low, we modified the fusion protocol as shown in Figure 11. The current-voltage relationship of membranes reconstituted using the above protocol is shown in Figure 12 (choline chloride as osmoticant), Figure 13 (potassium acetate as osmoticant) and Figure 14 (KCl as osmoticant). Figure 15 depicts a series of current-voltage curves with 400 mM KCl present in the *cis* side as osmoticant.

A general feature of the current-voltage curves depicted in Figures 12-15 is that, there is no true reversal potential. This is expected as choline chloride or potassium acetate or KCl which are used as osmoticants are not present in the *trans* side. The current-voltage curve approaches voltage axis asymptotically. The apparent reversal potential is between +80-120 mV. Since the potential differences are measured with respect to *trans* side as ground, the positive reversal potentials denotes appreciable chloride permeability through the reconstituted BLM.

In Search of an $InsP_3$-Gated and rynodine-sensitive Ca^{++} Channel in the Liver Rough ER Membrane

Figure 16 depicts the results of a typical experiment performed to look for $InsP_3$-gated Ca^{++} channels in the liver ER membrane. After fusion of a vesicle, the *cis* chamber was perfused with solution having a free Ca^{++} of 0.25 μM and the *trans* Ca^{++} level was raised to 23 mM. The conductance of the membrane dropped to about 30 pS. No Ca^{++} channels were seen when the membrane was

A.

cis *trans*

5 mM HEPES
1.3 mM $Ca(OH)_2$
or
6 mM PIPES
5.5 mM $Ca(OH)_2$
and 200 - 400 mM
Choline Chloride
or
Potassium acetate
or
Potassium Chloride

as osmoticant

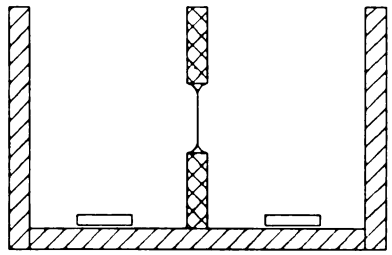

5 mM HEPES
1.3 mM $Ca(OH)_2$
or
6 mM PIPES
5.5 mM $Ca(OH)_2$

Perfuse cis side only and add an appropriate volume of a stock solution of HEPES + $Ca(OH)_2$ or PIPES + $Ca(OH)_2$ to raise the trans Ca^{++} concentration.

B.

cis *trans*

250 mM HEPES
140 mM TRIS
1 mM EGTA
0.5 mM $Ca(OH)_2$
or
60 mM PIPES
88 mM BTP
1 mM EGTA
0.5 mM $Ca(OH)_2$

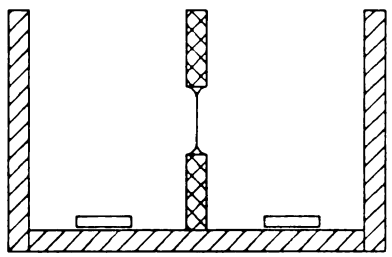

250 mM HEPES
55 mM $Ca(OH)_2$
or
60 mM PIPES
55 mM $Ca(OH)_2$

Figure 11. Modified schemes of the protocols for fusion of ER vesicles with a BLM (A) and recording of calcium channels (B).

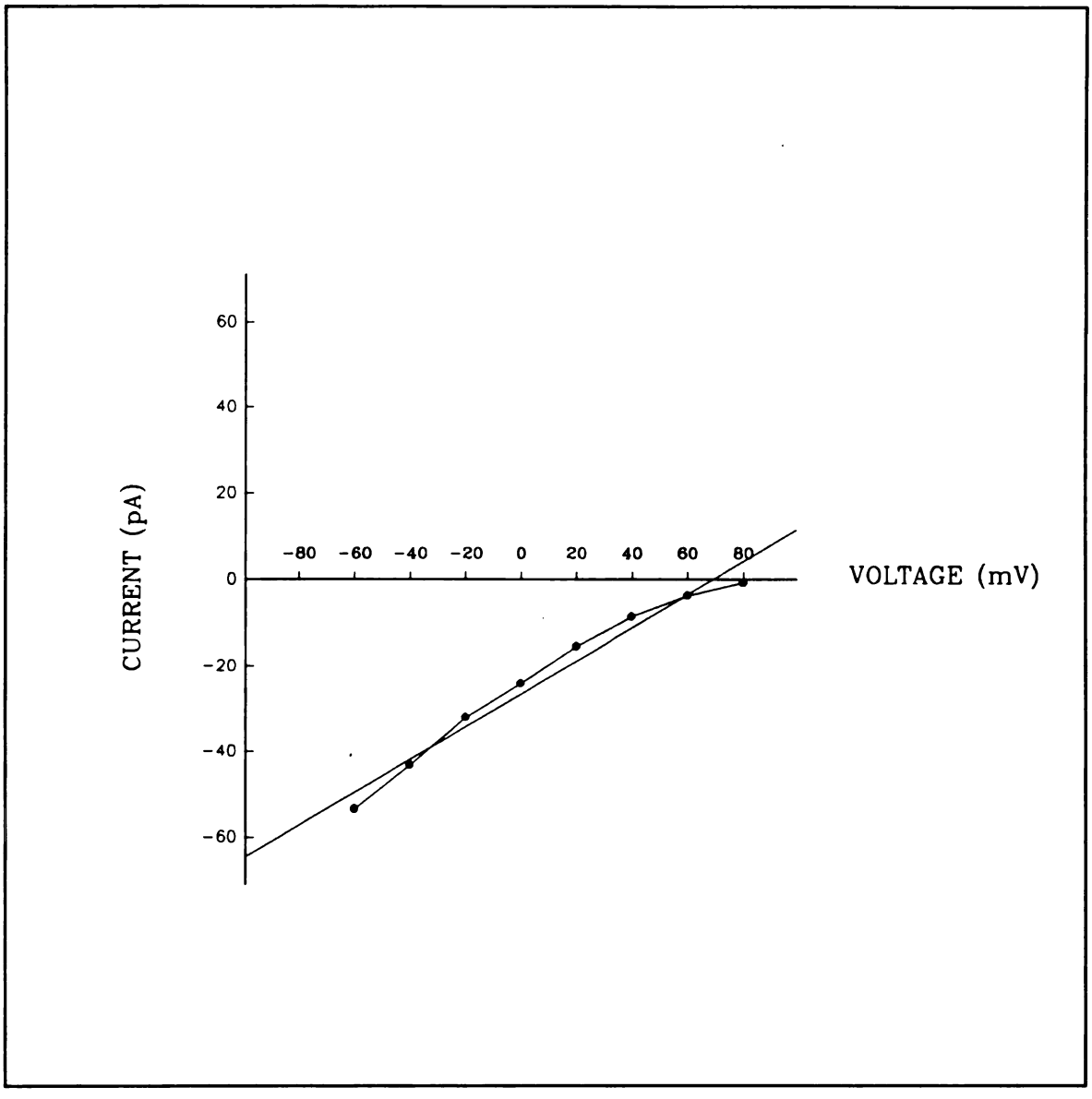

Figure 12. I-V curve of a BLM reconstituted with liver ER vesicles. The BLM was made in 11 mM PIPES + 10 mM $Ca(OH)_2$. Vesicles were made to fuse by adding choline chloride to the *cis* side (final concentration - 200 mM). After fusion, dc voltage steps were applied and current measured.

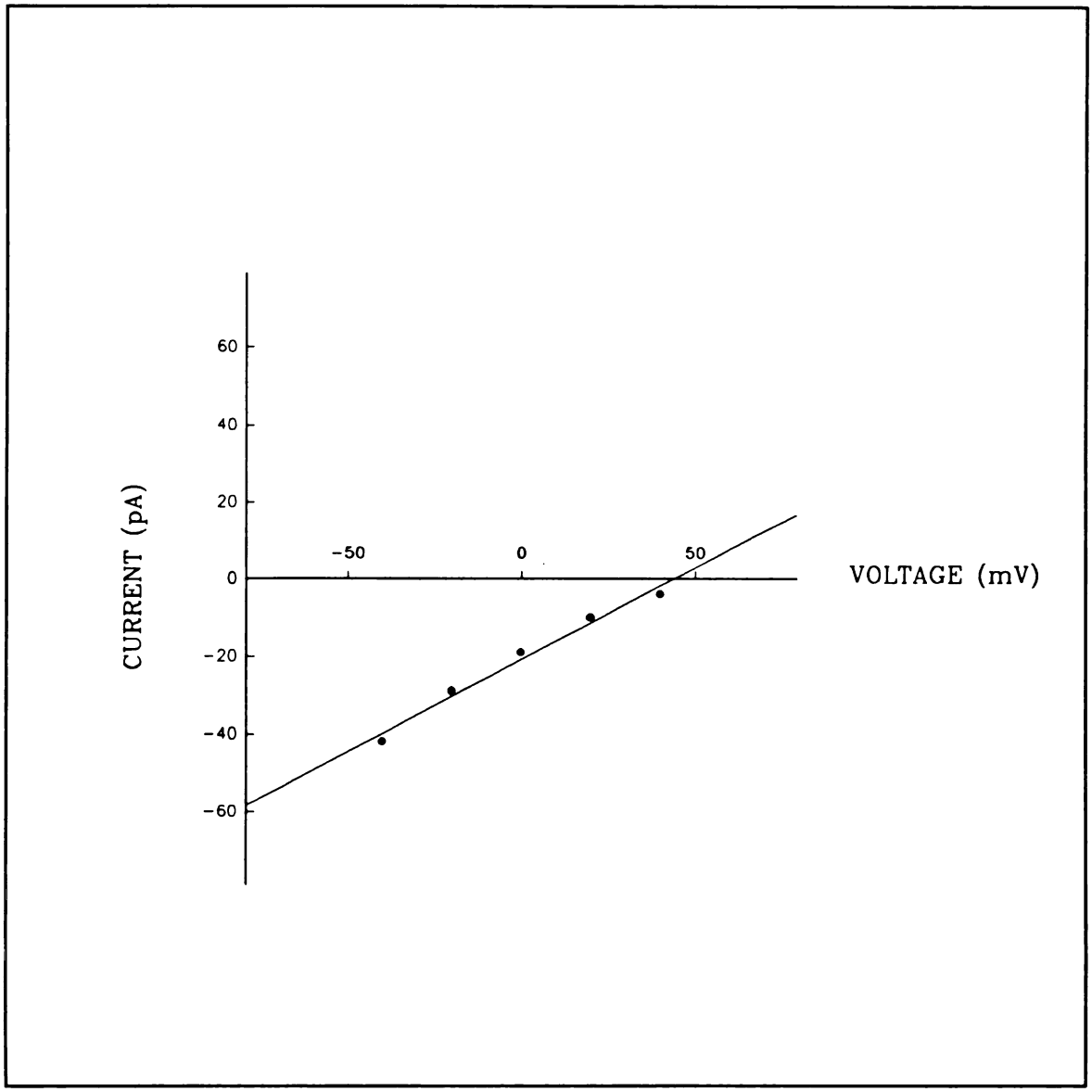

Figure 13. I-V curve of a BLM reconstituted with liver ER vesicles. The BLM was made in 5.5 mM PIPES + 5 mM $Ca(OH)_2$. Vesicles were made to fuse by adding potassium acetate to the *cis* side (final concentration - 200 mM). After fusion, dc voltage steps were applied and current measured.

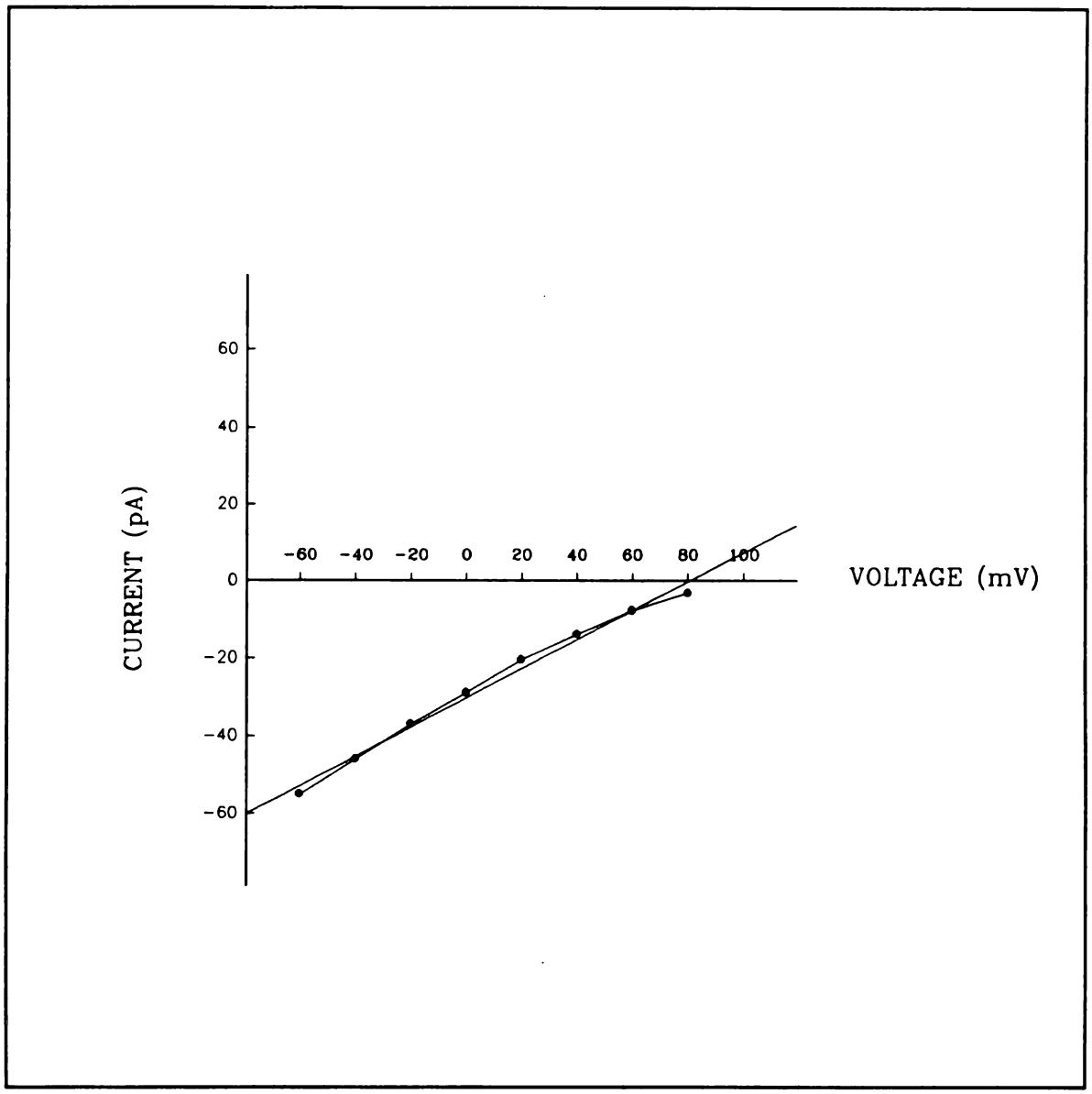

Figure 14. I-V curve of a BLM reconstituted with liver ER vesicles. The BLM was made in 5.6 mM PIPES + 5 mM $Ca(OH)_2$. After the BLM had completely thinned, potassium chloride was added to the *cis* side (final concentration - 300 mM) and ER vesicles (10 µg/ml) were added to the *cis* side. After fusion, dc voltage steps were applied and current measured.

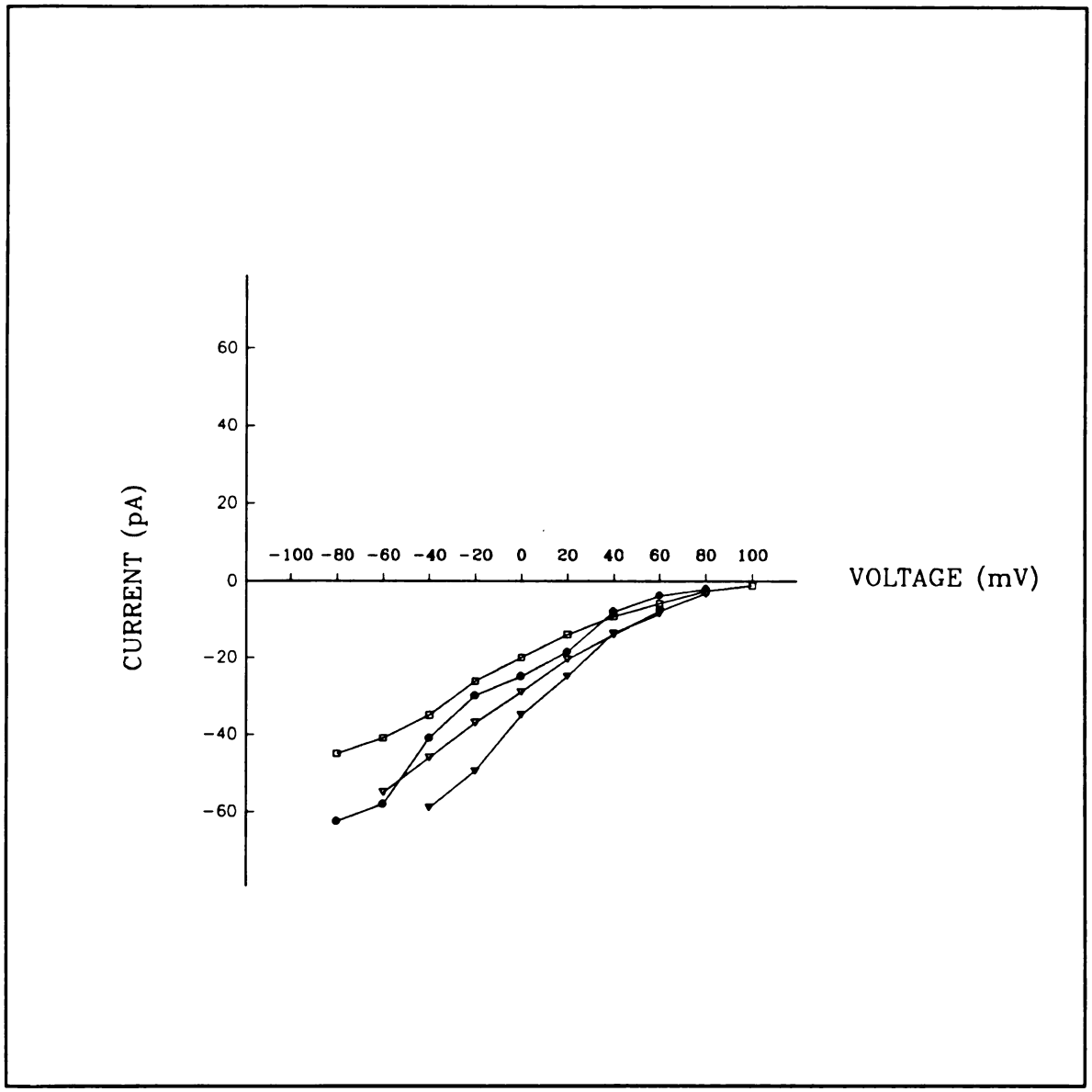

Figure 15. I-V curves of BLMs reconstituted with liver ER vesicles. The BLMs were made in symmetrical 20 mM HEPES + 4.5 mM $Ca(OH)_2$ solution. KCl solution was added to *cis* as osmoticant to induce fusion (final concentration - 400 mM). ER vesicles (10 µg/ml) were added to the *cis* side. After fusion, dc voltage steps were applied and current measured. Each symbol represents a different membrane.

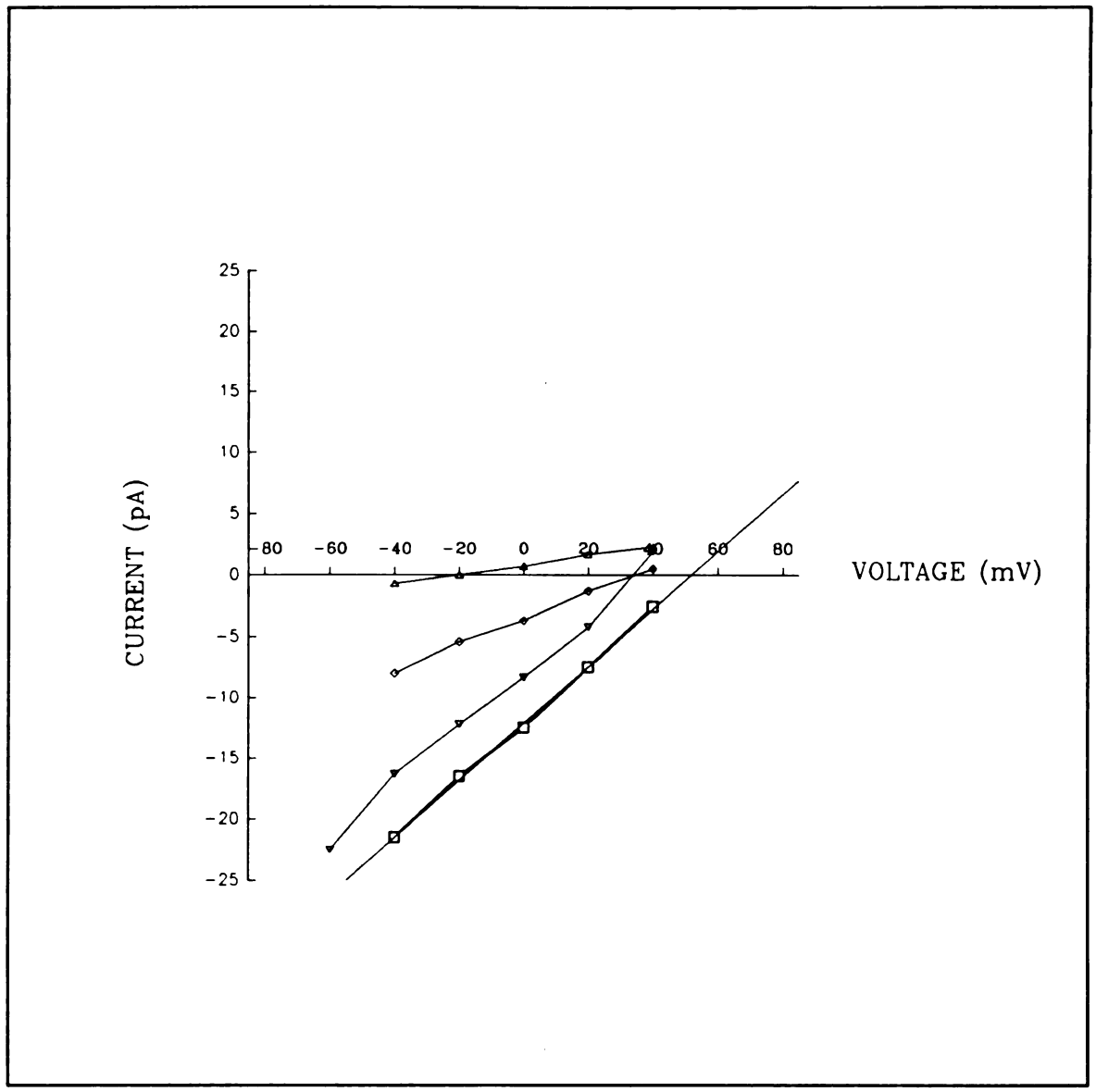

Figure 16. A typical reconstitution experiment to reveal any $InsP_3$-gated Ca^{++} channel present in the liver rough ER membrane. The BLM was made in symmetrical 6.25 mM PIPES + 5.6 mM $Ca(OH)_2$. Potassium acetate was added to the *cis* side as an osmoticant. The *cis* chamber was perfused after the fusion event with 25 mM PIPES + 38 mM BTP + 1 mM EGTA + 0.5 mM $Ca(OH)_2$ (0.25 µM free Ca^{++}) and the *trans* calcium level was raised to 23 mM. No calcium channels were observed when the membrane was challenged with 10µM $InsP_3$. □ - □, conductance of the reconstituted membrane; Δ - Δ, conductance after perfusion of *cis* chamber with 0.25 µM free calcium solution; ◊ - ◊, *cis* chamber contains 0.25µM free calcium + 50 mM potassium acetate; ∇ - ∇, *cis* chamber contains 0.25 µM free calcium + 100 mM potassium acetate.

challenged with 10 μM $InsP_3$. The membrane conductance to acetate remains intact however and it returns to the original level as the potassium acetate concentration is increased in the *cis* side. After repeated attempts (n - 100), We failed to detect any $InsP_3$-gated Ca^{++} channel in the liver ER membrane. We also failed to notice any rynodine-sensitive Ca^{++} channels though the appropriate concentrations of Ca^{++} (2.5 μM) and adenine nucleotides was present (data not shown)

Cl^- to K^+ Permeability Ratios of the ER Chloride Channels

We made reversal potential measurements in a number of experiments and P_{Cl^-}/P_{K^-} was calculated using the Goldman-Hodgkin-Katz equation in each case. The values (n = 36) are plotted in the form of a histogram in Figure 17. The results indicate that the P_{Cl^-}/P_{K^-} values vary from 4 to 24. If P_{Cl^-}/P_{K^-} is one of the characteristic properties of a channel, the results indicate that there are many different types of Cl^- channels having different P_{Cl^-}/P_{K^+} values. Another alternative interpretation is that there are at least two types of channels; one type having a low P_{Cl^-}/P_{K^+} (4-8) and the other a high P_{Cl^-}/P_{K^+} (20-24) and the in-between values are different combinations of these two types of channels.

Permeability Ratios of Halides and Other Anions

Figure 18 depicts a typical current-voltage curve of a reconstituted membrane having initially 402 mM KCl on the *cis* side and 2 mM KCl on the *trans* side. The reversal potential is gradually shifted toward zero mV, when KBr solution is added to the *trans* side. It can clearly be seen from the figure that Br^- is more permeable than Cl^- as 281 mM KBr in the trans side can counter-balance 402 mM KCl in the cis side. A $\frac{P_{Br^-}}{P_{Cl^-}}$ value can be calculated in this case,

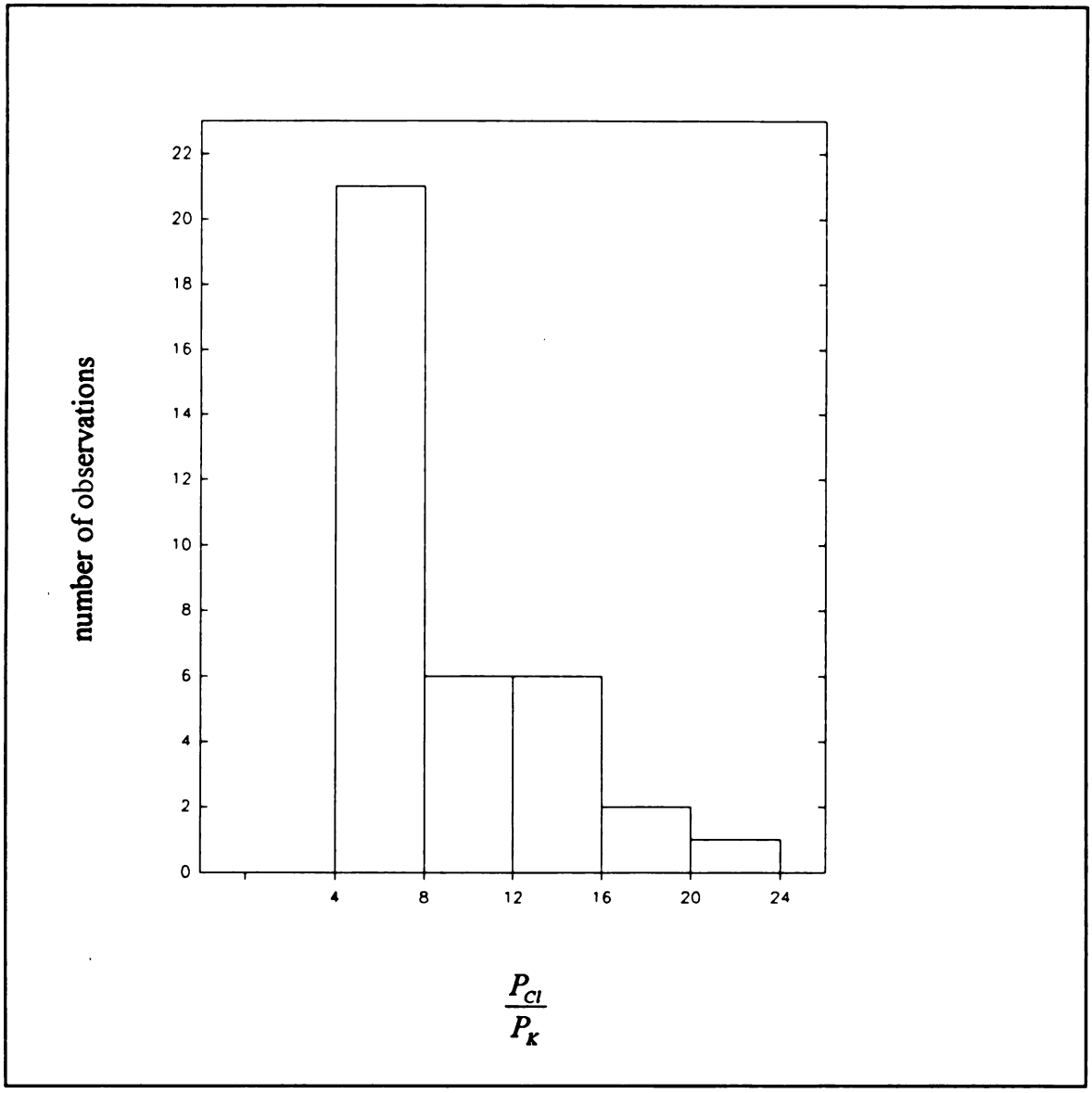

Figure 17. Histogram of P_{Cl}^{-} / P_K^{+} values. Each value was obtained by reversal potential measurement in bi-ionic condition and calculated using the Goldman-Hodgkin-Katz equation.

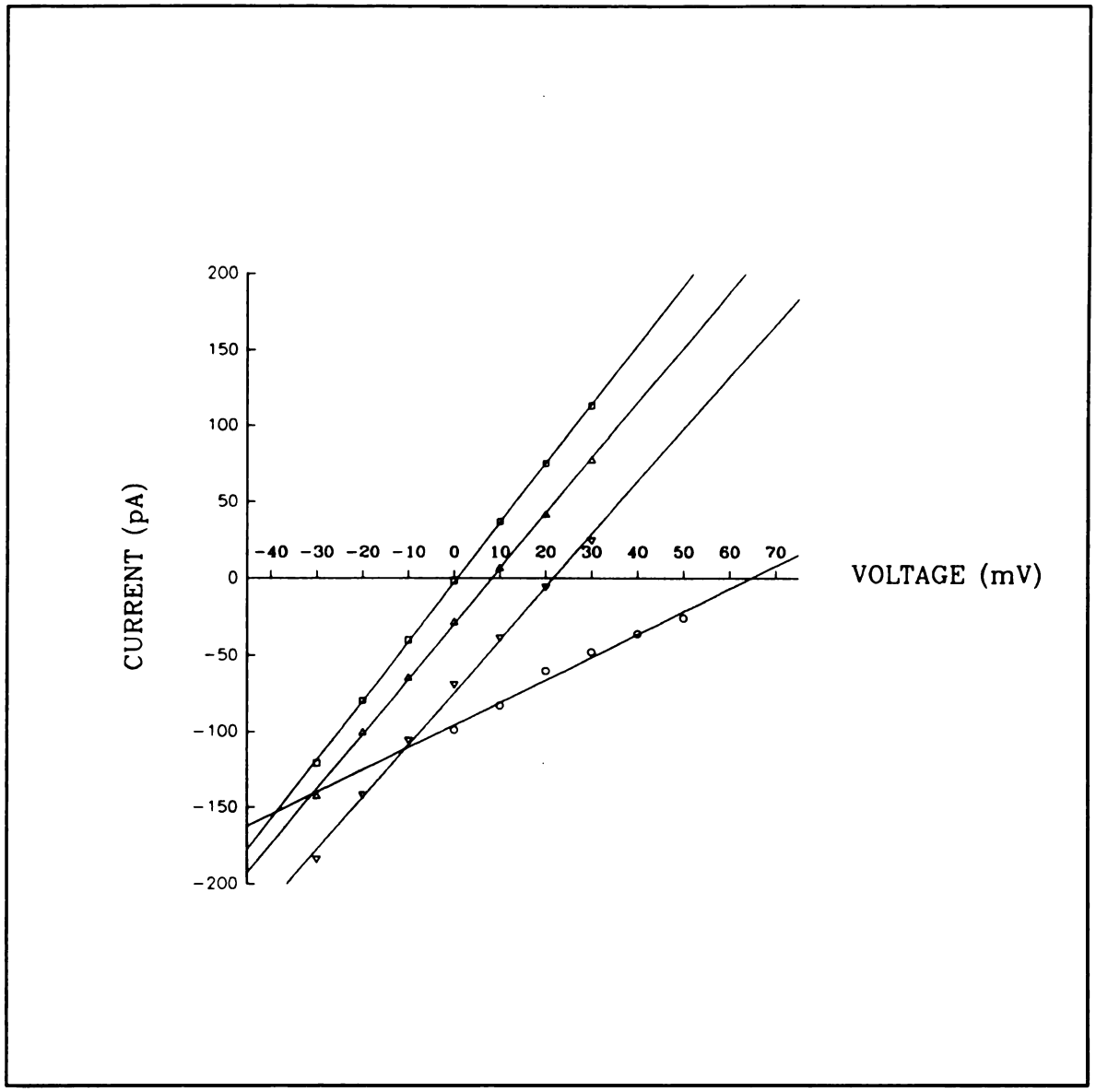

Figure 18. Reversal potential measurement under near bi-ionic conditions (KCl *cis* side and KBr *trans* side) across a BLM reconstituted with liver ER vesicles. O-O, *cis* chamber contains 5 mM HEPES + 1 mM $Ca(OH)_2$ + 402 mM KCl, *trans* chamber 5 mM HEPES + 1 mM $Ca(OH)_2$ + 2 mM KCl; ∇-∇, *cis* same as above, *trans* 5 mM HEPES + 1 mM $Ca(OH)_2$ + 100 mM KBr; Δ-Δ, *cis* same as above, *trans* 5 mM HEPES + 1 mM $Ca(OH)_2$ + 193 mM KBr; ; □ -□, *cis* same as above, *trans* 5 mM HEPES + 1 mM $Ca(OH)_2$ + 281 mM KBr.

using the Goldman-Hodgkin-Katz equation and including K^+, Cl^- and Br^- as permeant ions. Figure 19 shows the results of a similar experiment, but having K^+, Cl^- and iodide as the permeant ions. I^- is even more permeable than Cl^-, as can be seen from the figure. A reversal potential of -8mV is obtained when the *trans* side contains 187 mM KI and the *cis* side contains 365 mM KCl. Using the Goldman-Hodgkin-Katz equation, a value for $\frac{P_{I^-}}{P_{Cl^-}}$ can be calculated. Figure 20 shows the results of an experiment in which K^+, Cl^- and SCN^- are the permeant ions. A reversal potential of +3 mV is obtained when the *trans* side contains 88 mM KCNS; the *cis* side contains 274 mM KCl and one can calculate a value for $\frac{P_{SCN^-}}{P_{Cl^-}}$. Figure 21 shows the results of a control experiment in which SCN^-, Cl^- and K^+ are the ion species present, but the membrane is an unmodified one. Figure 22 is a current-voltage curve of a control experiment in which the ionic species present are K^+, Cl^- and I^-. In this control experiment the KI solution was one day old and one can see significant current across the BLM. As iodide is permeable through the BLM it is important that KI solution should be prepared immediately before use.

Table 1 is a compilation of $P_{test\ anion}/P_{Cl^-}$ values and the Pauling diameters of the test anions taken from Hille (87). The anionic selectivity sequence follows the sequence SCN^- (2.68) > I^- (1.68) > Br^-(1.32) > Cl^- (1) > gluconate$^-$ (0.11). $P_{test\ anion}/P_{Cl^-}$ is calculated using activities based on available activity coefficients taken from Robinson and Stokes (91).

Table 2 shows the compilation of $P_{test\ anion}/P_{Cl^-}$ values from the present study and taken from literature for lobster neuron (70), mouse GABA-and glycine-activated Cl^- channel (47), SR Cl^- channel (63) and cAMP-activated

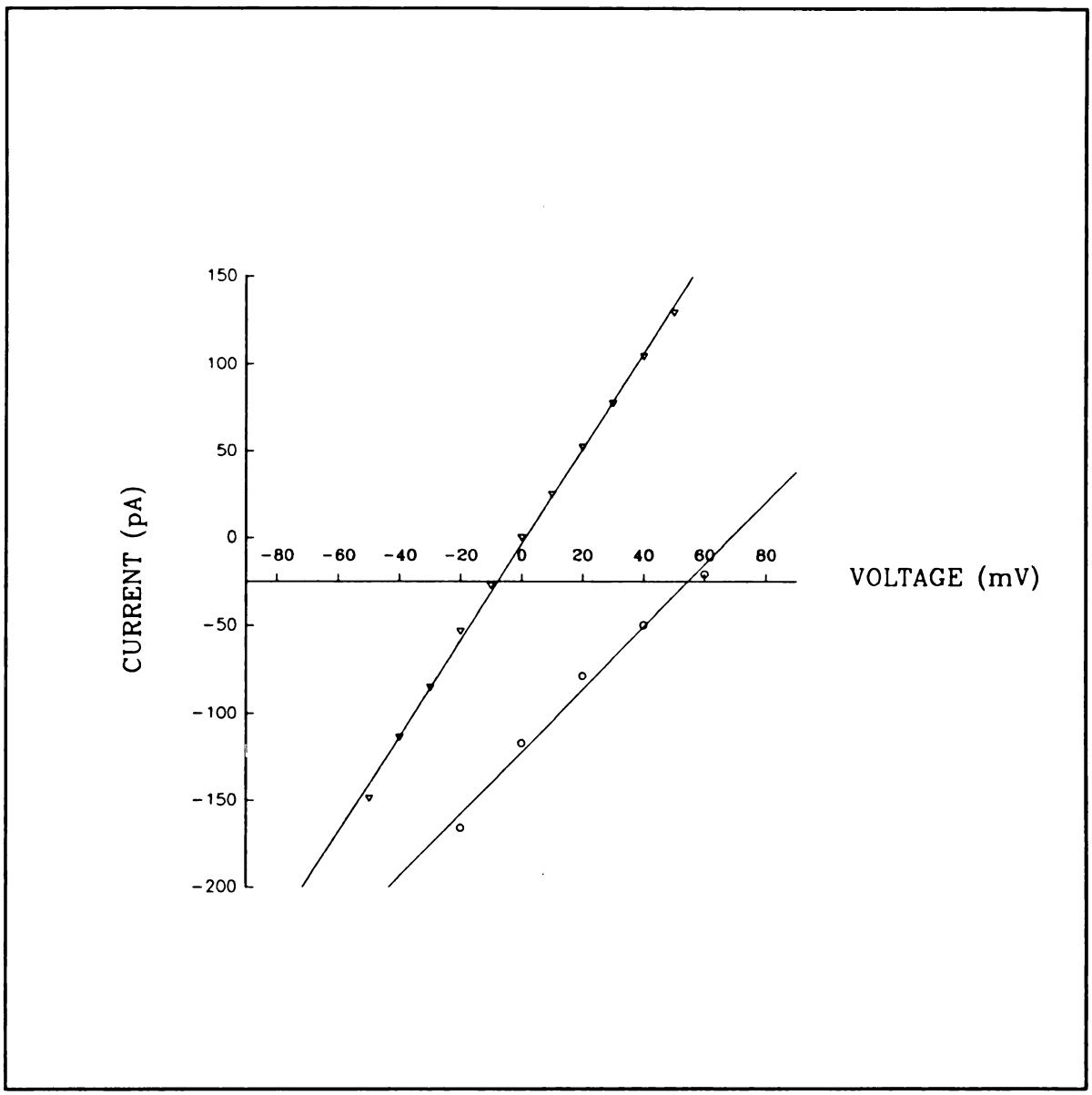

Figure 19. Reversal potential measurement under near bi-ionic condition (KCl *cis* side and KI *trans* side) across a BLM reconstituted with liver ER vesicles. In O-O, the *cis* chamber contains 5mM HEPES + 1 mM $Ca(OH)_2$ + 365 mM KCl and the *trans* chamber 5mM HEPES + 1 mM $Ca(OH)_2$ + 2 mM KCl; ∇-∇, *cis* chamber contained the same solution as above and the *trans* chamber contained 5mM HEPES + 1 mM $Ca(OH)_2$ + 187 mM KI;

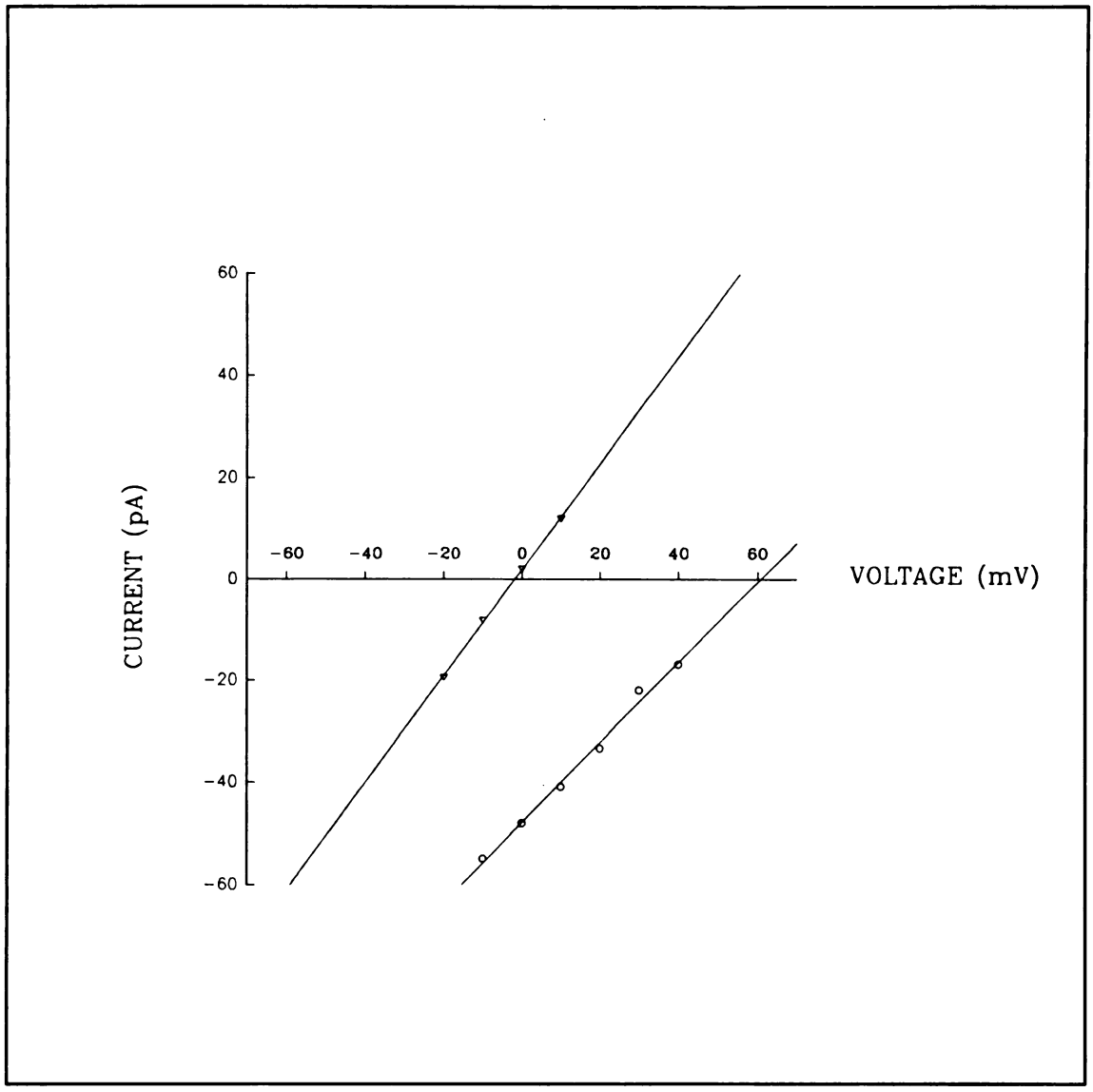

Figure 20. Reversal potential measurement under near bi-ionic condition (KCl *cis* side and KCNS *trans* side) across a BLM reconstituted with liver ER vesicles. In O-O, the *cis* chamber contains 5mM HEPES + 1 mM $Ca(OH)_2$ + 274 mM KCl and the *trans* chamber 5mM HEPES + 1 mM $Ca(OH)_2$ + 2 mM KCl; ∇-∇, the *cis* chamber contained the same solution as above and the *trans* chamber contained 5mM HEPES + 1 mM $Ca(OH)_2$ + 88 mM KCNS.

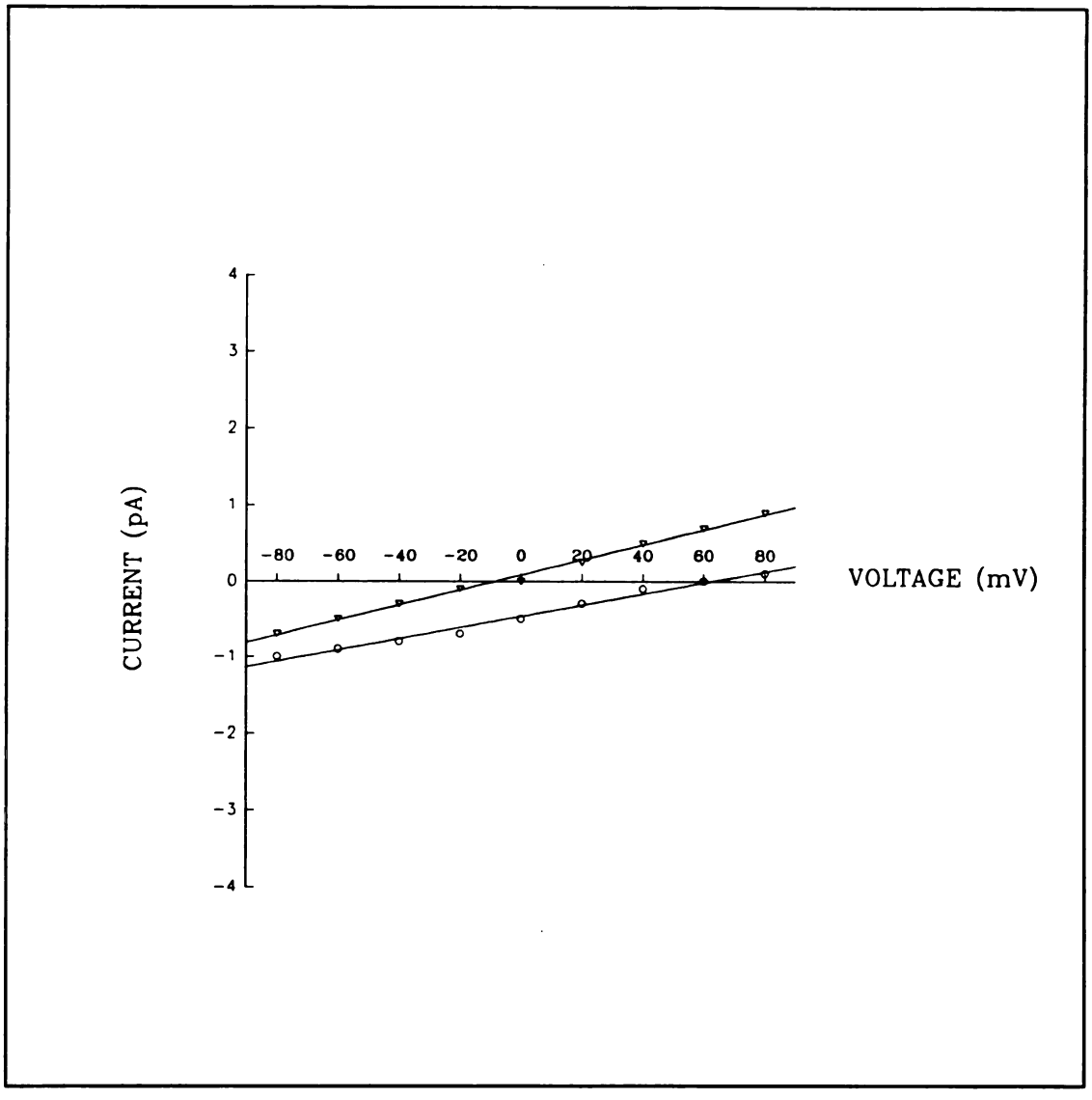

Figure 21. A control experiment for bi-ionic potential measurement (KCl *cis* side and KCNS *trans* side) using an unmodified BLM. In O - O , both the *cis* and *trans* chambers contain 5 mM HEPES + 1 mM $Ca(OH)_2$ + 2 mM KCl, ∇ - ∇, the *cis* chamber contains 363 mM KCl and the *trans* chamber 187 mM KCNS.

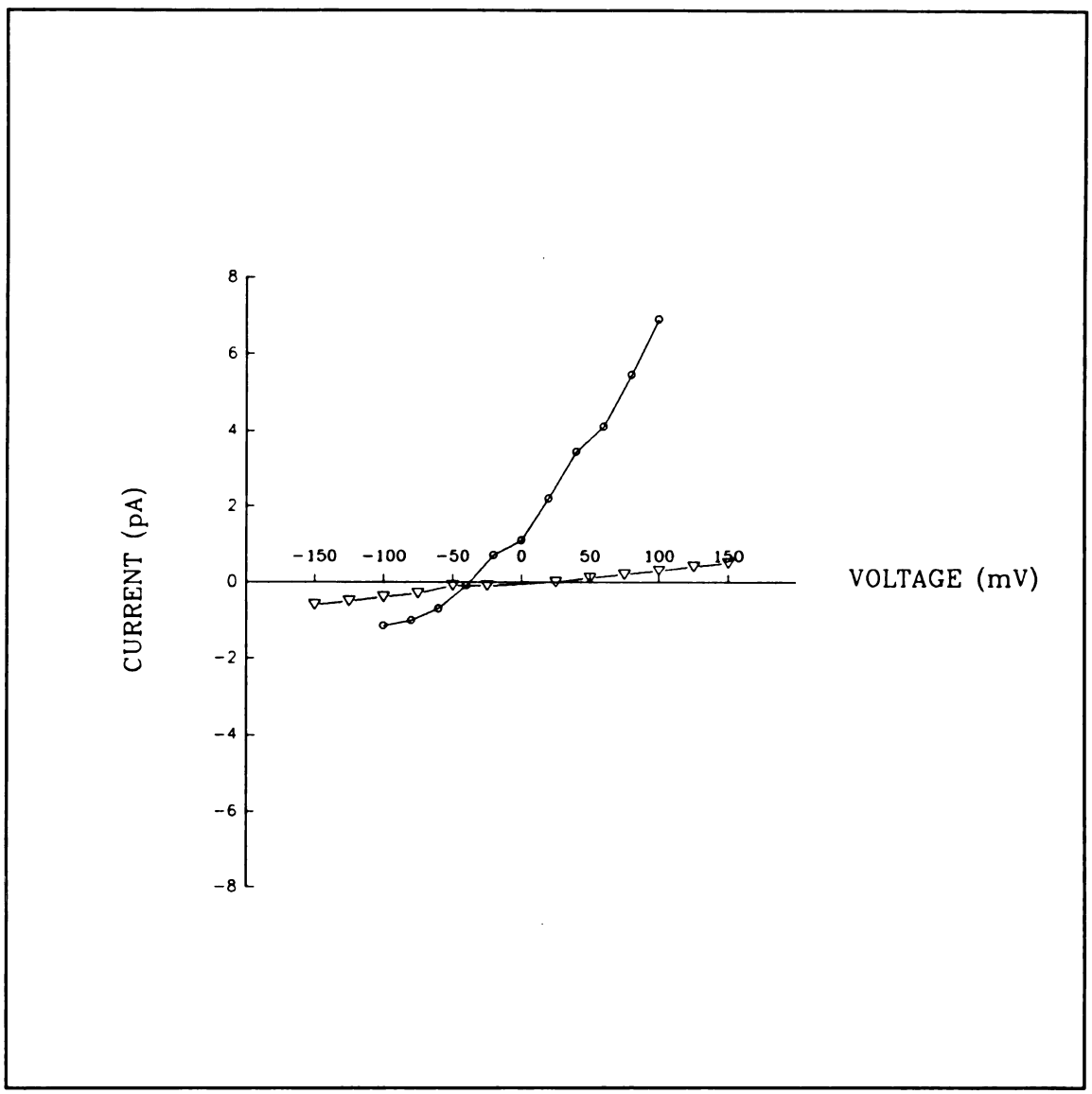

Figure 22. A control experiment for bi-ionic potential measurement (KCl *cis* side and KI *trans* side) using an unmodified BLM. In ∇-∇, the *cis* and the *trans* chambers contain 5mM HEPES + 1 mM $Ca(OH)_2$ + 2 mM KCl; O-O, the *cis* chamber contains 363 mM KCl and the *trans* chamber 214 mM KI.

Table 1. Anionic Permeability Ratios of ER Chloride Channels. Reversal potentials in this study were determined under near bi-ionic conditions in which the *cis* chamber contained KCl and the *trans* chamber the test anion. Permeability ratios were calculated using the Goldman-Hodgkin-Katz equation. Anion diameters for halides are taken from Hille (87).

Test ion	Diameter(A)	n	P_{test} / P_{Cl^-}
SCN^-	3.6 (1.9)	5	2.68
I^-	4.3	2	1.68
Br^-	3.9	5	1.32
Cl^-	3.6	--	1
$Gluconate^-$	6.0	1	0.11

Table 2. Anionic Permeability Ratios for Different Chloride Channels. Reversal Reversal potentials in this study were determined under near bi-ionic conditions in which the *cis* chamber contained KCl and the *trans* chamber the test anion. Permeability ratios were calculated using the Goldman-Hodgkin-Katz equation. The listed permeability ratios for lobster neuron; mouse Gly-R, GABA-R; CFTR and SR Cl- channels are from literature. n.d. - not determined.

	P_{test}/P_{Cl^-}						
Test ion	Lobster neuron	Gly-R	GABA-R	CFTR	CFTR (K95D)	SR	Present study
Ref.	(70)	(47)	(47)	(48)	(48)	(63)	
SCN^-	n.d.	n.d	n.d.	n.d.	n.d.	1.45	2.68
I^-	2.70	1.80	2.80	0.59	1.43	1.39	1.68
Br^-	1.50	1.40	1.50	1.11	1.25	1.00	1.32
Cl^-	1.00	1.00	1.00	1.00	1.00	1.00	1.00
Gluconate	0.06	n.d.	n.d.	n.d.	n.d.	0.04	0.11

cystic fibrosis Cl^- channel (48). So, our Ptest anion / P_{Cl^-} values, though measured under macroscopic conditions, compare favorably with those of Cl^- channels in other systems. According to the terminology of Eisenman's selectivity theory (92), the liver ER vesicular Cl^- channel(s) exhibits a low field-strength permeability sequence for halides in which lower dehydration energy of the larger anions predominates over stronger coulombic interaction energy of smaller anions in determining selectivity. This selectivity behavior is different from that of the Cl^- channel from *Torpedo californica* (56) and the cystic fibrosis Cl^- channel (48).

Inhibition of Cl^- Conductance by Zn^{++} and DIDS

Since some Cl^- channels are inhibited by Zn^{++}, we studied the effect of Zn^{++} on the macroscopic Cl^- conductance of a BLM reconstituted with liver ER vesicles. Figure 23 shows the macroscopic Cl^- conductance blocked in increasing order by increasing concentrations of $ZnCl_2$ added to *cis* and *trans* sides and the conductance block finally reaches saturation. Under our experimental conditions, 3.5 mM $ZnCl_2$ was sufficient to block all Zn-sensitive conductance.

Table 3 is a compilation of the Cl^- conductances blocked by saturating concentrations of $ZnCl_2$. As can be seen from the table, saturating concentrations of $ZnCl_2$ can block sometimes totally and sometimes partially, the Cl^- conductance of the BLMs reconstituted with ER vesicles. This suggests that some of the vesicles which fuse with the BLM have only Zn-sensitive Cl^- conductances and some others have additional Zn-insensitive Cl^- conductances.

Since many anion transport systems and channels are inhibited by disulfonic acid stilbene derivatives, we studied the effect of DIDS (4,4'-diisothiocyanostilbene-2,2'-disulfonic acid) on the macroscopic Cl^- conductance

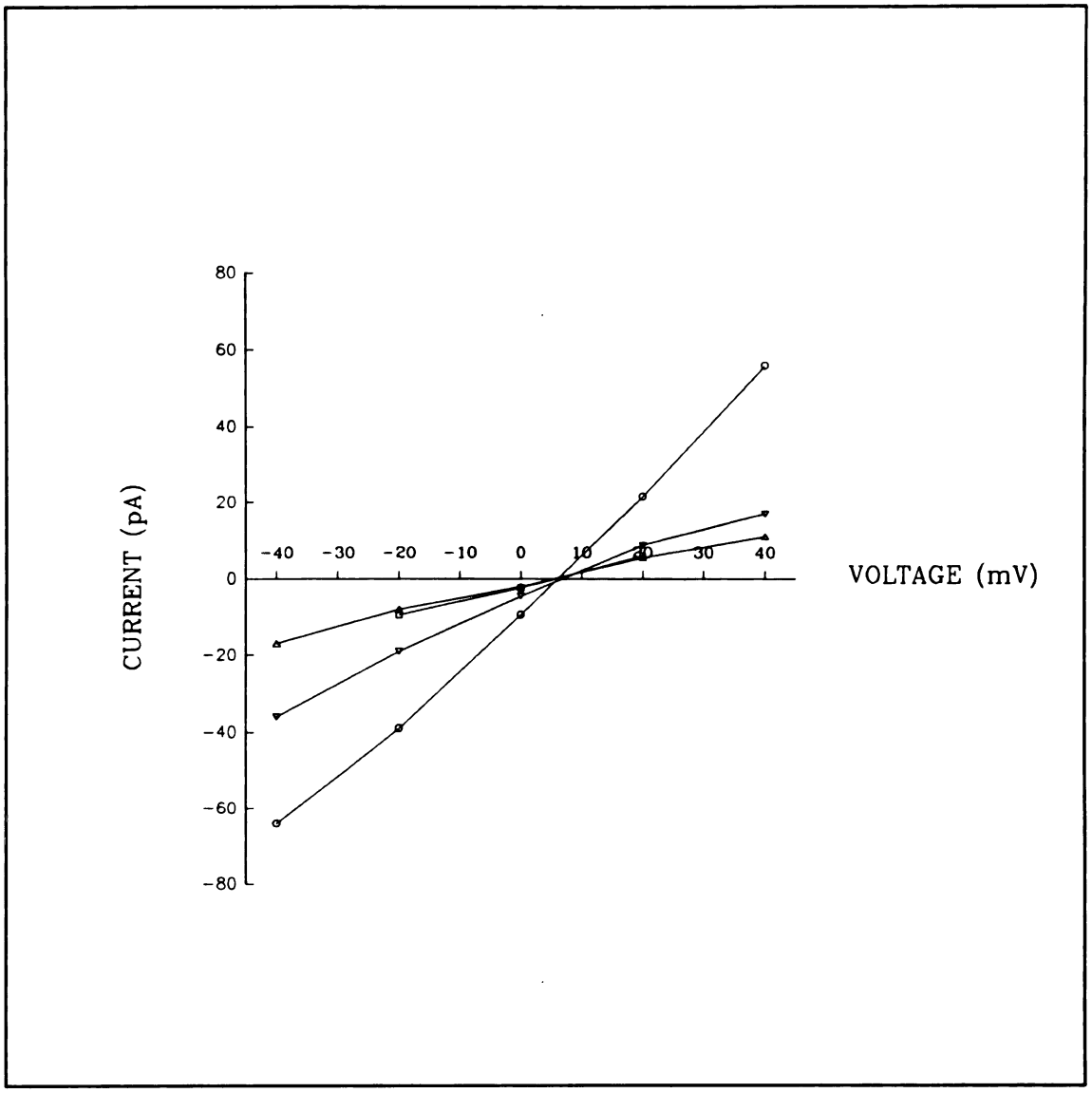

Figure 23. Decrease in macroscopic conductance after addition of $ZnCl_2$: I-V curve of a BLM reconstituted with liver ER vesicles. The BLM was made in symmetrical 5.5 mM HEPES + 1 mM $Ca(OH)_2$. Fusion was initiated by adding KCl solution to the *cis* side to a final concentration of 363 mM. After fusion, the osmotic gradient was eliminated by adding KCl solution to the *trans* side. O - O, no $ZnCl_2$; ∇- ∇, 0.875 mM $ZnCl_2$ to *cis* and *trans* sides; Δ - Δ, 1.75 mM $ZnCl_2$ to *cis* and *trans* sides; □ - □, 3.5 mM $ZnCl_2$ to *cis* and *trans* sides;

Table 3 Inhibition of Macroscopic Chloride Conductance by Zn^{++}. Numbers in parentheses in the left column indicate KCl concentration in mM across the BLM (*cis/trans*). The values in the second column indicate the conductance blocked by Zn^{++}. Columns 3 and 4 describe a possible breakdown to unit channel conductance. "Mean unit conductance" taken from the experiments in which both *cis* and *trans* KCl concentration was 363 mM are: 0.283 ± 0.011 pS or 0.589 ± 0.039 pS (mean ± s.d.).

Initial Conductance (nS)	**Conductance Blocked by Zn^{++} (nS)**		
1.502(363/363)	1.154	0.288×4	0.577×2
0.594(363/363)	0.594	0.279×2	0.594×1
0.572(363/363)	0.572	0.286×2	0.572×1
0.570(363/363)	0.570	0.285×2	0.570×1
1.114(363/363)	1.114	0.279×4	0.557×2
1.329(363/363)	1.329	0.265×5	0.665×2
0.341(410/210)	0.341	0.341×1	0.341×1
1.924(181/181)	1.434	0.239×6	0.478×3
1.832(181/181)	1.832	0.240×4	0.480×2
Mean ± s.d.		**0.283 ± 0.011**	**0.589 ± 0.039**

of the reconstituted BLM. Figure 24 shows a typical result of the effect of DIDS on the macroscopic Cl^- conductance. In this particular case, 36 μM DIDS blocked 75 percent of the Cl^- conductance; the rest could not be blocked by increasing the DIDS concentration up to 840 μM. This suggests that some of the ER vesicles in addition to having some DIDS-sensitive conductance, have a residual DIDS-insensitive conductance.

Table 4 is a compilation of Cl^- conductance values that are blocked by at least 40 μM of DIDS. It is clear from the table that DIDS, in some cases, cannot block all the Cl^- conductance. In about 95 percent of the cases, we found that DIDS block occurred from *cis* side.

Next, we studied the effect of DIDS and $ZnCl_2$ together on the macroscopic Cl^- conductance of a BLM reconstituted with liver ER vesicles. Figure 25 is a typical example of the effect of both DIDS and Zn^{++} added sequentially. 36 μM DIDS blocked about 60 percent of the macroscopic Cl^- conductance. We then added 2mM $ZnCl_2$ which inhibited another 33 percent of the macroscopic Cl^- conductance.

Next, we studied the effect of DIDS and $ZnCl_2$ in the reverse order, by first adding $ZnCl_2$ and then DIDS. Figure 26 is an example of such an experiment, in which, after the membrane was reconstituted with liver ER vesicles, 2.7 mM $ZnCl_2$ was added to *cis* and *trans* sides. About 25 percent of the conductance was inhibited. Adding 18 μM of DIDS to the *cis* side further eliminated about another 60 percent of conductance.

Studies at the Level of Single Channel

These studies were very difficult to carry out. We followed the usual procedure of dilution and sonication of the ER vesicular sample. Since it is known that the ER vesicles aggregate upon dilution, the diluted and sonicated

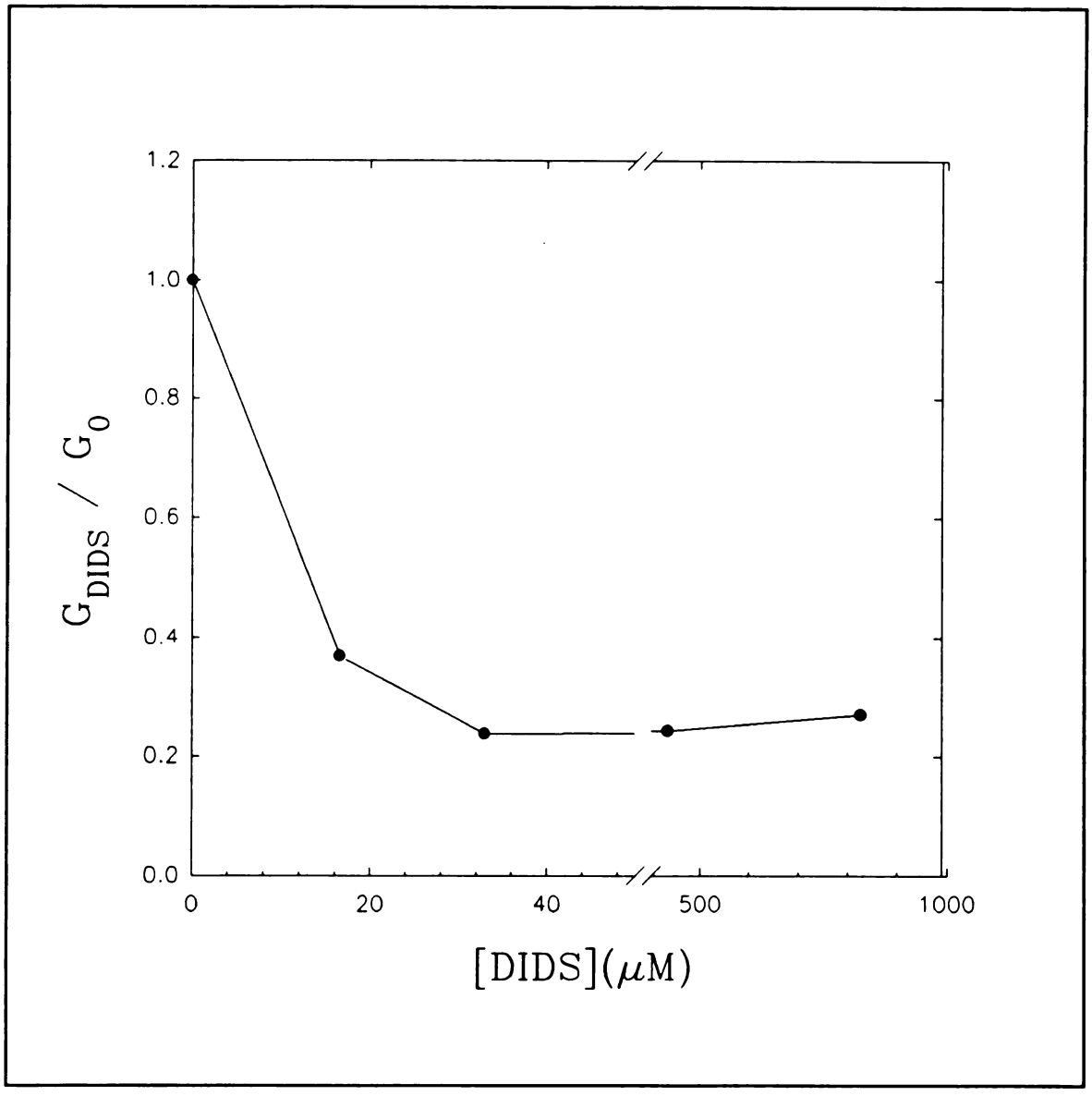

Figure 24. Inhibition of macroscopic chloride conductance by DIDS. After reconstituting a BLM with liver ER vesicles, different concentrations of DIDS were added to the cis side and the conductance of the membrane was determined.

Table 4. Inhibition of Macroscopic Chloride Conductance by DIDS. Numbers in the left column indicate the initial conductance. The values in the second column indicate the conductance blocked by DIDS. Columns 3 and 4 describe possible breakdown to unit channel conductance. "Mean unit conductance" are: 0.566 ± 0.021 pS or 0.190 ± 0.005 pS (mean ± s.d.).

Initial Conductance (nS)	**Conductance Blocked by DIDS (nS)**		
2.467	1.138	0.569×2	0.189×6
2.898	1.784	0.594×3	0.198×9
1.437	1.069	0.534×2	0.182×6
0.584	0.565	0.565×1	0.188×3
2.178	0.567 (blocked from the trans side)	0.567×1	0.189×3
2.178	0.766 (blocked from the trans side)	0.766×1	0.191×4
mean±s.d.		**0.566± 0.021**	**0.190± 0.005**

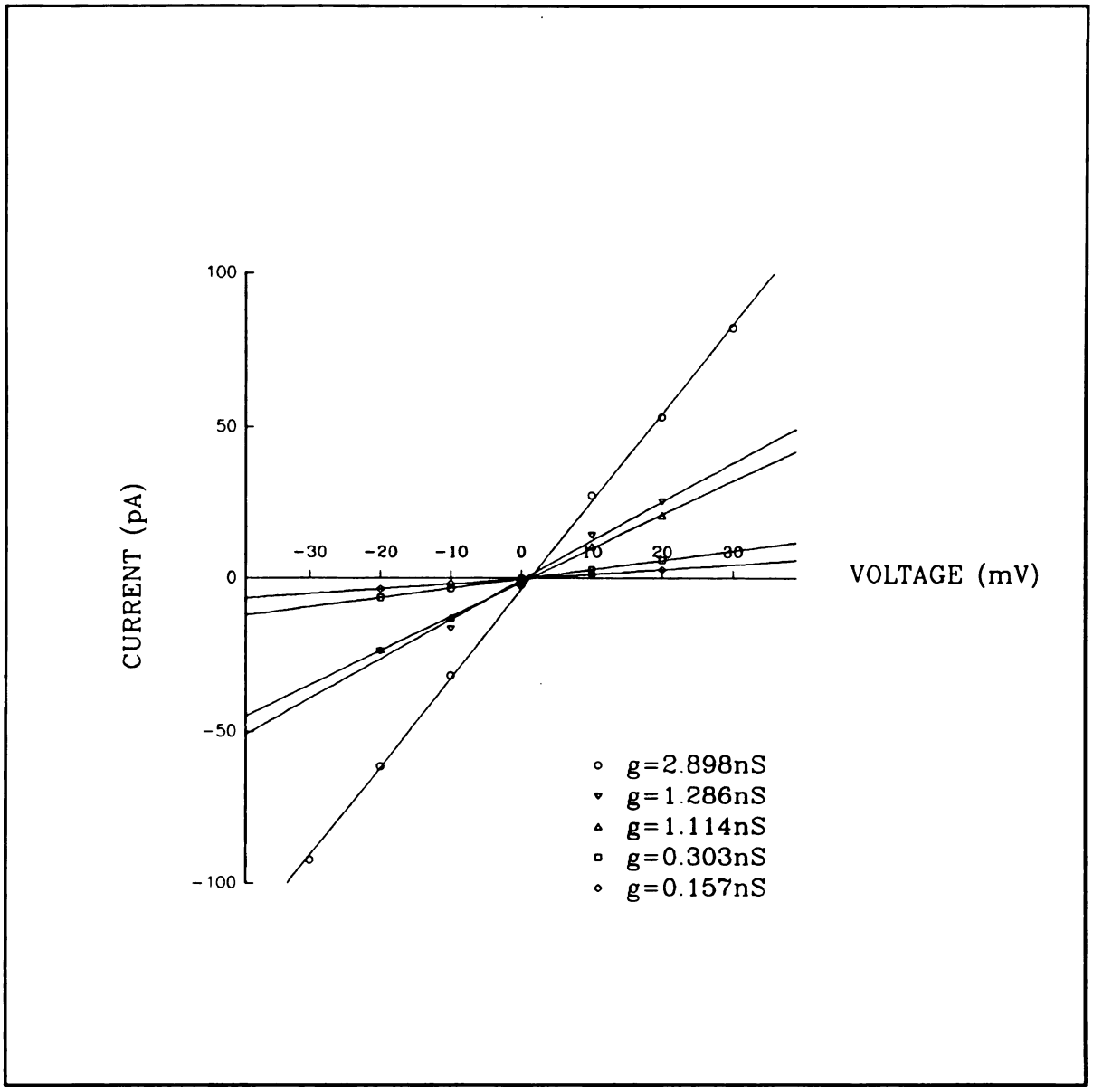

Figure 25. Effect of DIDS and $ZnCl_2$ on macroscopic chloride conductance of a BLM reconstituted with liver ER vesicles. The BLM was made in symmetrical 5mM HEPES + 1 mM $Ca(OH)_2$ + 2 mM KCl. Fusion of the vesicles with the BLM was initiated by adding 363 mM KCl to the *cis* side. After reconstitution, the osmotic gradient was eliminated by raising the *trans* KCl concentration. O-O , after reconstitution; ∇-∇,18 µM DIDS to both *cis* and *trans* sides; Δ-Δ, 36 µM DIDS to both *cis* and *trans* sides; □-□, 0.5 mM $ZnCl_2$ to both *cis* and *trans* sides; ◊-◊, 2 mM $ZnCl_2$ to both *cis* and *trans* sides.

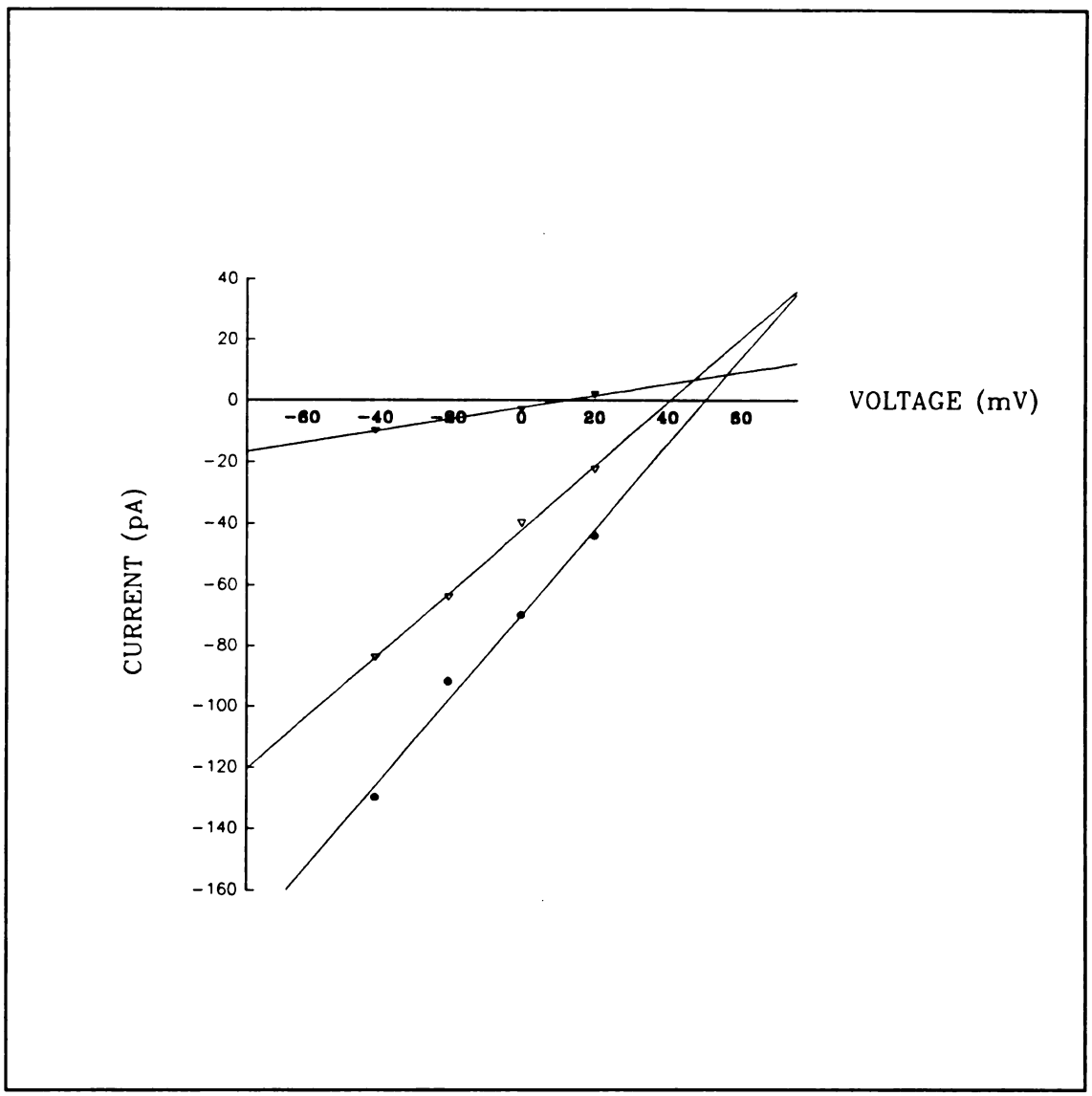

Figure 26 Inhibition of conducatnce by Zinc (Zn^{++}) and DIDS: Conductance of a BLM reconstituted with liver vesicales (○ - ○ 1.4nS); Conducatance after the addition of 2.7 mM $ZnCl_2$ to the *cis* and *trans* sides (● - ● 1.04 nS); Conducatance after addition of DIDS to the *cis* side (∇ - ∇ 0.192 nS).

sample probably aggregate again when added to the *cis* chamber. In our fusion experiments, the minimum conductance which we observed in 363 mM symmetrical KCl solution was between 550-600 pS. Some of these conductances could be totally eliminated by DIDS (n = 2), and in some cases (n = 2), the single channel activity could be eliminated totally by $ZnCl_2$. Figure 27 shows some of our single channel records in symmetrical 363 mM KCl solution. A maximum conductance transition of 200 pS an many other transition lower than this value can be seen. Addition of 38 μM DIDS totally eliminated all activity. Figure 28 shows another set of single channel records in which the channel activity could be eliminated by addition of $ZnCl_2$.

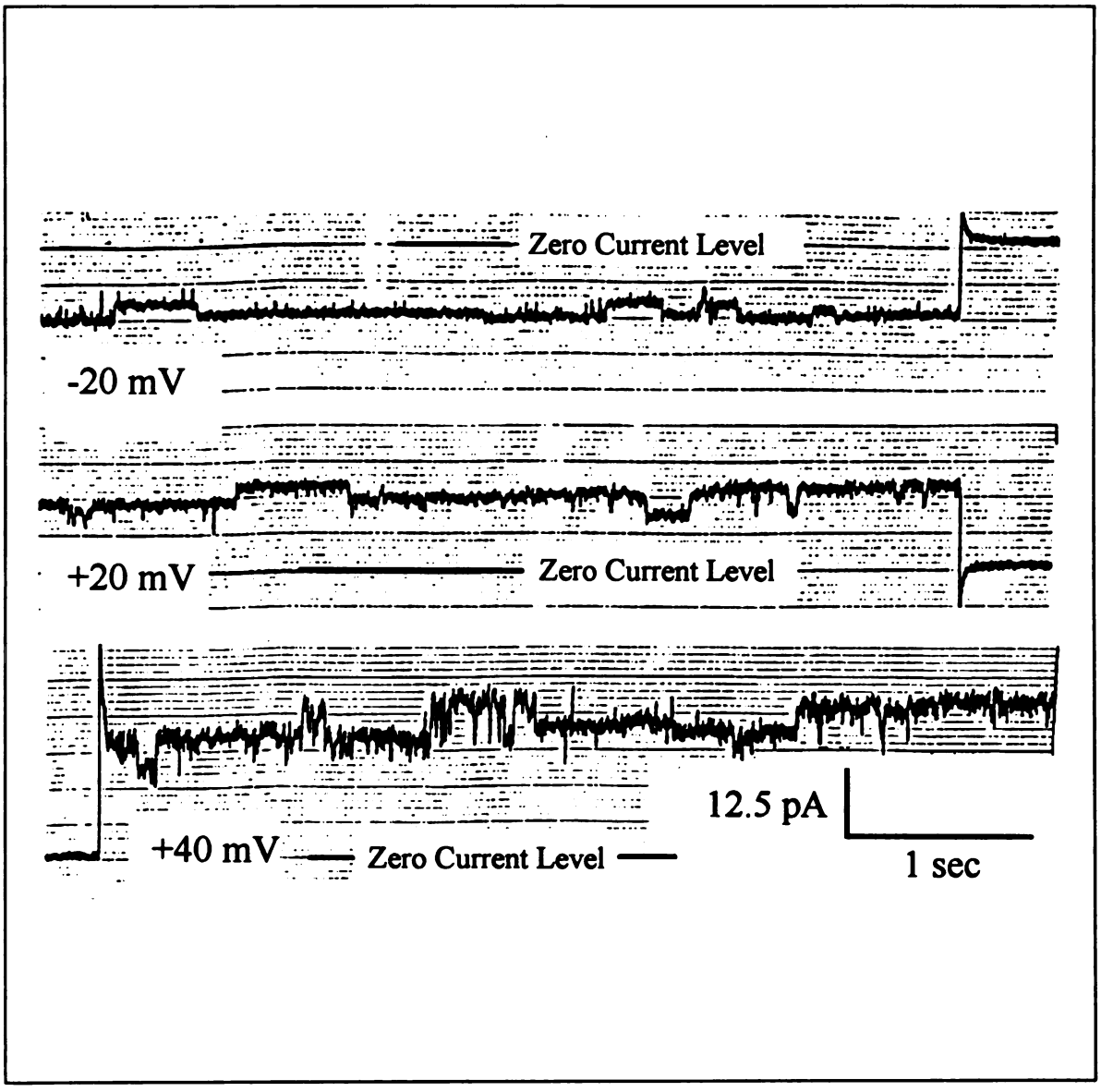

Figure 27 Single channel activity observed in a planar BLM reconstituted with liver rough ER vesicles. The bathing solution is symmetrical 363 mM KCl. The holding voltages are given near each trace. The channel activity could be eliminated by addition of DIDS.

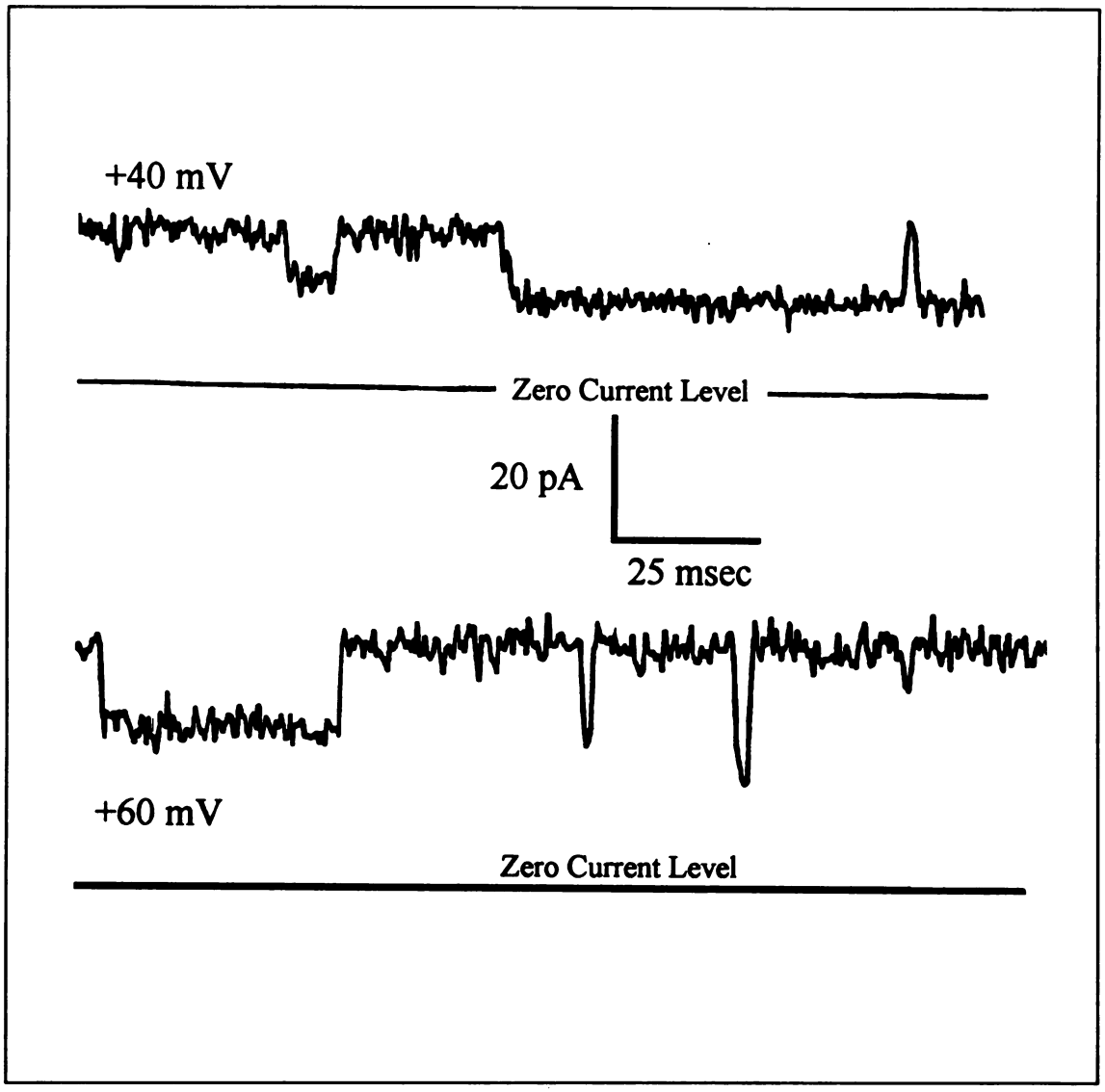

Figure 28 Single channel activity observed in a planar BLM reconstituted with liver rough ER vesicles. The bathing solution is symmetrical 363 mM KCl. The holding voltages are given near each trace. The channel activity could be eliminated by addition of $ZnCl_2$.

DISCUSSION

Fusion of ER Vesicles with a BLM

In asymmetric choline chloride solution, the ER vesicles could be fused with a BLM. Since the reversal potential is 25 mV, when *cis* and *trans* choline chloride concentrations are 250 and 50 mM, respectively, the fusion of ER vesicles imparts appreciable Cl^- conductance to the BLM. The above protocol was used for the fusion of SR vesicles (32) with a BLM. In the above case, the vesicles fused such that the *cis* side of the BLM is the cytoplasmic side and the *trans* is the luminal side of the SR. In other studies (35,36), in which cerebellar ER vesicles were fused with a BLM, the *cis* side was equivalent to the cytoplasmic side and *trans* side was the luminal side. Consequently, we assumed that the liver ER vesicles will fuse with the same orientation and accordingly, we perfused the *cis* side with a solution having very low free Ca^{++} (0.25 μM or 2.5 μM) and the *trans* side 55 or 23 mM Ca^{++}.

The above fusion protocol has the drawback, that in order to give the Ca^{++} gradient across the reconstituted BLM, both the *cis* and *trans* chambers have to be perfused and in our hands the success rate of having an intact BLM after perfusing both the chambers being low, we have modified the above protocol and have used one in which the perfusion of the *cis* chamber only is necessary to impose a Ca^{++} gradient across a reconstituted BLM. Our experimental results demonstrate that it is possible to make BLMs in low ionic strength solutions and that choline chloride, potassium acetate and KCl can be used as osmoticants to fuse liver ER vesicles with a BLM.

In Search of $InsP_3$-gated and rynodine-sensitive Ca^{++} Channels in Liver Rough ER Membrane

Though we made repeated attempts and maintained appropriate conditions (Ca^{++} concentration, agonist $InsP_3$ concentration), we were unable to detect any $InsP_3$-gated Ca^{++} channel in the liver rough ER membrane. $InsP_3$-gated Ca^{++} channels have been observed in planar BLM after fusion of cerebellar ER vesicles. So, our inability to observe $InsP_3$-gated Ca^{++} channels in planar BLM after fusion of liver ER vesicles suggests that the $InsP_3$ receptor/channel is not located in liver ER. In this regard, we can cite a recent study (30) in which distribution of $InsP_3$ binding sites was investigated in subcellular fractions obtained from rat liver and compared with those of other markers. It was found that $InsP_3$ binding vesicles were completely distinct from the ER derived vesicles and co-purified with the plasma membrane marker. Though the rynodine-sensitive Ca++ channels have been observed in planar BLMs after fusion of total brain microsomes (35) and cerebellar microsomes (36), our inability to observe these channels after fusion of liver rough microsomes suggests that the channel is probably not located in the liver rough ER membrane. As mentioned earlier one study (39) has shown that in liver only the smooth microsomal membranes are enriched in rynodine binding sites.

Cl^- to K^+ Permeability Ratios for Liver Rough ER Chloride Channels

By imposing an asymmetric KCl solution across BLMs reconstituted with liver ER vesicles, we measured the reversal potential in each case, and applying a form of Goldman-Hodgkin-Katz (GHK) equation, we calculated P_{Cl^-}/P_{K^+} in each case. The calculated values vary from 4 to 24. To explain this variation, we assume that there exist Cl^- channels in the ER with different P_{Cl^-}/P_{K^+}

values, and in macroscopic condition, what we measure, is a weighted average of the P_{Cl^-}/P_{K^+} values of all the channels that have got incorporated in the BLM.

Mathematically, the GHK equation for three ionic species (K^+, Na^+ and Cl^-) is as follows:

$$E_{rev} = \frac{RT}{F} \ln \frac{P_{K^+}[K^+]_O + P_{Na^+}[Na^+]_O + P_{Cl^-}[Cl^-]_i}{P_{K^+}[K^+]_i + P_{Na^+}[Na^+]_i + P_{Cl^-}[Cl^-]_o}$$

If we have only K^+ and Cl^-, then the equation can be reduced to:

$$E_{rev} = \frac{RT}{F} \ln \frac{P_{K^+}[K^+]_O + P_{Cl^-}[Cl^-]_i}{P_{K^+}[K^+]_i + P_{Cl^-}[Cl^-]_o}$$

Dividing the numerator and denominator by P_K, we obtain:

$$E_{rev} = \frac{RT}{F} \ln \frac{[K^+]_O + \frac{P_{Cl^-}}{P_{K^+}}[Cl^-]_i}{[K^+]_i + \frac{P_{Cl^-}}{P_{K^+}}[Cl^-]_o}$$

And if in a particular reconstituted BLM, we have many Cl^- channels with differing P_{Cl^-}/P_{K^+} ratios, we can write a modified GHK equation for this case as follows:

$$E_{rev} = \frac{RT}{F} \ln \frac{[K^+]_O + \left(\frac{P_{Cl^-}}{P_{K^+}}\right)_{w.a.}[Cl^-]_i}{[K^+]_i + \left(\frac{P_{Cl^-}}{P_{K^+}}\right)_{w.a.}[Cl^-]_o}$$

where

$$\left(\frac{P_{Cl^-}}{P_{K^+}}\right)_{w.a.} \equiv \frac{n_1\left(\frac{P_{Cl^-}}{P_{K^+}}\right)_1 + n_2\left(\frac{P_{Cl^-}}{P_{K^+}}\right)_2 + n_3\left(\frac{P_{Cl^-}}{P_{K^+}}\right)_3 + \ldots n_m\left(\frac{P_{Cl^-}}{P_{K^+}}\right)_m}{n_1 + n_2 + n_3 + \ldots n_m}$$

and n_1 = number of channels having $\frac{P_{Cl}}{P_K}$ ratio $\left(\frac{P_{Cl}}{P_K}\right)_1$

n_2 = number of channels having $\frac{P_{Cl}}{P_K}$ ratio $\left(\frac{P_{Cl}}{P_K}\right)_2$

and so on.

To give a concrete example, if we have at least two types of channels, one type having P_{Cl^-}/P_{K^+} between 4 and 8 and the other type having P_{Cl^-}/P_{K^+} of 20-24 and if in a membrane, we have only one type, we measure a P_{Cl^-}/P_{K^+} of 4-8 or 20-24. If we have one channel of one type and one channel of the other type, we would expect a P_{Cl}/P_K of 12-16. The range of P_{Cl}/P_K values that we have obtained, we believe, can be explained in this way.

Anionic Permeability Ratios

At the outset, we must mention that our anionic permeability ratios are measured under macroscopic conditions. So, if we have different channel types, the selectivity sequence should hold good for all the Cl^- channel types. The permeability sequence is $SCN^- > I^- > Br^- > Cl^-$ suggesting that the Cl^- channels present in the liver rough ER membrane have "low field-strength sites," following Eisenman's terminology (92). The gluconate permeability of the ER Cl^- channels seems to be a little higher than other Cl^- channels and is about one-tenth of the Cl^- permeability. Since the ionic diameter of gluconate is 6 A°, we

can assign a value, slightly greater than 6 °A as the diameter of the Cl^- channels.

We also studied the permeability of a few other anions and cations. Acetate permeability was almost the same as that of Cl^-, fluoride permeability less than that of Cl^-. Sulfate seemed impermeable and sodium was about half as permeable as K^+. (Data not shown for the above cases.)

No K^+ "Channel" in the ER Membrane

Meissner et al. had studied the permeability of various anions and cations using a potentiometric dye (2). From their studies, they concluded that though majority of the liver microsomes are more permeable to K^+ and Na^+ than to Mg^{++} or Ca^{++}, they lacked a highly conducting K^+ and Na^+ channel structure, such as the K^+ and Na^+ channel of sarcoplasmic reticulum. In our studies of direct fusion of liver ER vesicles with a BLM, we were unable to find any K^+ channel.

Inhibition of Chloride Conductance by DIDS and Zinc

We found that the Cl^- conductance of the rough liver ER membrane can be divided into two components based on their pharmacological sensitivity. One component can be blocked by DIDS.and the other component by Zn^{++}

<u>Inhibition by DIDS</u>

The reactive disulfonic acid stilbenes (DIDS and 4-acetamide-4'-isothiocyanotostilbene-2,2'-disulfonic acid, SITS) block some Cl^- channels including a voltage-gated conductance studied macroscopically in squid giant axon (93) and astrogalia (94), the low conductance channel of *Torpedo* electroplax (56), rabbit urinary bladder (59), lobster neuron (70) and the large

conductance channels of A6 epithelial cells (61)and B lymphocytes (95). In many of these cases, DIDS was active from the cytoplasmic side. DIDS in 1 μm concentration inhibited irreversibly the macroscopic Cl^- conductance induced by the *Torpedo* vesicles (56). Inhibition of lobster neuronal Cl^- channel by SITS could be fitted to a one-site blocking behavior with a K_I of 53 μM (70).

In our experiments, 36 μM of DIDS can inhibit sometimes totally and sometimes partially the Cl^- conductance induced by liver rough ER vesicles. We interpret our findings as follows:

There are two types of Cl^- channels in the liver ER membrane. One type can be blocked by DIDS, which we shall call DIDS-sensitive, and the other DIDS-insensitive. During physical disruption of the intact ER (as happens during isolation of ER vesicles), we get a non-homogeneous population of ER vesicles. Some of the vesicles carry the DIDS-sensitive Cl^- channels, some DIDS-insensitive type and some both types. That is why in our studies involving the inhibition of Cl^- conductance by DIDS what we observe amounts to what type of vesicles have fused with the BLM. If a vesicle carrying DIDS-sensitive type channels only has fused with the BLM, we can inhibit the entire conductance by DIDS. If a vesicle carrying DIDS-insensitive type channels have fused with the BLM, we cannot eliminate it by DIDS (we shall show later that the conductance insensitive to DIDS can be blocked by zinc). If both types of vesicles have fused or the third type carrying both DIDS-sensitive and DIDS-insensitive channels have fused with the BLM, then by application of DIDS, we can inhibit only the DIDS-sensitive portion of the total conductance. In this regard, it is interesting to note that it has been our observation that when the vesicle induced conductance is small (indicating that only one vesicle has fused), the conductance is fully DIDS-sensitive type or DIDS-insensitive type. When the vesicle induced

conductance is large (indicating many fusion events), the conductance can be partially eliminated by DIDS.

Sidedness of DIDS Block

As has been mentioned earlier, in many of the studies involving DIDS inhibition of Cl^- channels, DIDS was active from the cytoplasmic side. In about 95% of our experiments, DIDS blocked the DIDS-sensitive Cl^- conductance from the *cis* side. To induce fusion with the BLM, we add the ER vesicles to the *cis* side. During isolation, if the ER vesicles maintain their normal orientation (we have no reason to believe that it would be otherwise), then, when the vesicle fuses with the BLM, the *trans* side shall be equivalent to the luminal side of the ER and the cis side equivalent to the cytoplasmic side. So, we can say that, in our case, DIDS blocks from the cytoplasmic side.

Inhibition by Zinc

In frog skeletal muscle, external zinc decreases Cl^- efflux (96,97) and reduces Cl^- conductance with a K_I near 0.1 mM (98,99). Thus, there is evidence that 0.1-2 mM zinc in the extracellular solution blocks Cl^- channels of intact muscle. In a recent study of a high-conductance anion channel in adult amphibian skeletal muscle, it was found that 10 mM zinc inhibited the channel activity but DIDS or 9-anthracene-carboxylic acid (another blocker of Cl^- channel) had no effect (60).

In our studies, we found that 2.5 mM zinc can eliminate totally or partially, the conductance induced by ER vesicles. In cases which the inhibition was partial, there was no further inhibition by increasing zinc concentration and the residual conductance could be blocked by DIDS. We interpret our data in an analogous way as we have done for the DIDS case.

We conclude that the liver ER has two types of Cl^- channels: one type that we shall call DIDS-sensitive and zinc-insensitive, the other type is DIDS-insensitive and zinc-sensitive.

Single Channel Studies

Single channel studies were difficult to perform in our case. In some cases, we noticed that the single channel activity could be completely eliminated by DIDS (n = 2) and in some other cases (n = 2), the single channel activity could not be eliminated by DIDS but by zinc. Since "n" is very small, it is not possible for us to draw any definite conclusions about the single channel properties of the DIDS-sensitive and zinc-sensitive channels. We shall limit ourselves to only our observations.

Minimum Conductance Induced by ER Vesicle Fusion with a BLM

The minimum conductance that we observed in 363 mM symmetrical KCl solution was between 550-600 pS. This most likely is due to fusion of a single vesicle. Sometimes this "minimal" conductance could be eliminated by DIDS and if it could not be eliminated by DIDS, it could be eliminated by addition of zinc.

Minimal Conductance of a DIDS-Sensitive Channel

Since, in our fusion experiment, the minimum conductance that we observed which could be blocked by DIDS is about 565 pS, and if this is a "minimal" conductance of the DIDS sensitive channel, we wanted to see if at the macroscopic level, the conductance that could be blocked by DIDS is an integer multiple of this "minimal" conductance. In 5 out of 6 cases (Table 4), the conductances can be shown to be an integer multiple of a minimal conductance

of 0.566± 0.021 nS (mean ± s.d.). The minimal conductance that we observed in our fusion experiments is around this value. As mentioned earlier, this minimal conductance is, most probably, due to fusion of one vesicle. But is it one channel? It is possible that the vesicle may be carrying more than one channel. In that case, the unit conductance of the channel would be lower than 0.566 nS.

We, then looked at our single channel records in which the minimal conductance of 0.566 nS could be totally inhibited by application of 38μM DIDS to the cis side. The maximum conductance transition that we observed was about 200pS and many other transitions occurred which were smaller than this value. We again looked at our macroscopic conductances which could be blocked by DIDS. In all 6 cases, the conductances can be shown to be integer multiples of a "minimal" conductance of 192pS. Is this the unit conductance of a DIDS-senstive channel? We do not know. As mentioned earlier our 'n' is too small to draw any definite conclusions. Further experiments are necessary to clarify this point.

Minimal Conductance of a Zinc-Sensitive Channel

In this case also, 'n' being small (n=2), we cannot draw any definite conclusions and shall limit ourselves to our observations.

The minimal conductance that we observed (which could not be blocked by DIDS, but could be blocked by subsequent addition of zinc was about 600pS. We believe that this is probably due to fusion of a single vesicle. But is it the unit conductance of a single zinc-sensitive channel? It is possible that the single vesicle could be carrying more than one channel. In that case, the unit conductance would be lower than 600pS.

We looked at the macroscopic Cl^- conductance which could be inhibited by zinc. As in the DIDS case, we wanted to see if the macroscopic conductance

could be shown to be an integer multiple of a "minimal" conductance of about 600pS. Since the conductance is a function of salt concentration, we selected those values in which the *cis* and *trans* KCl concentrations were 363 mM. In all 5 of such cases, the "minimal conductance" comes out to be 0.589 $\pm$ 0.0399nS (Table 3).

We looked at two records in which single channel activity could be blocked by zinc. There were multiple transitions. There were conductance transitions of magnitude 75pS, 150pS, 225pS, 300pS and 375pS. We could not come to any definite conclusion about the unit conductance from our single channel studies. Further experiments are necessary to clarify this point.

Physiological Significance of ER Cl^- Channels

We are unable to state the exact physiological function of these channels. We can only offer speculations. Since the SR is a specialized derivative of ER and a high conductance Cl^- channel has been identified in the SR membrane, we decided to see if the proposed functions for the SR Cl^- channel should offer us any clues. For the SR channel it has been proposed that a possible function of this anion channel could be to shorten the time course of the Ca^{++} transient and produce a faster twitch. Another physiological function proposed is to provide counter-ion movement during Ca^{++} pumping (100) after the SR Ca^{++} release channels have closed. We know that Ca^{++} is sequestered in the ER. A Ca^{++}-ATPase and a Ca^{++} binding protein calreticulin have been identified in the liver ER. Since Ca^{++} pumping is electrogenic, we believe that the physiological role of the ER anionic channels may be to provide counter ion movement into the ER, so as to prevent build up of positive charges inside the ER.

SUMMARY

1. The liver rough ER vesicle imparted high chloride conductance to the BLM after fusion.

2. Cl^- to K^+ permeability ratios measured under macroscopic conditions varied from 4 to 24.

3. Anionic permeability follows the sequence $SCN^- > I^- > Br^- > Cl^- >>>$ gluconate which suggests that the the chloride channels have low field-strength sites.

4. The gluconate$^-$ permeability was observed to be one-tenth of that of Cl^- permeability. This suggests that the diameter of the rough ER chloride channel(s) is slightly larger than 6 Å.

5. The macroscopic Cl^- conductance could be pharmacologically dissected to DIDS-sensitive and Zn^{++}-sensitive types.

6. In most cases DIDS blocked Cl^- conductance from the *cis* side (the side to which the ER vesicles are added; equivalent to the cytoplasmic side of the ER).

7. The minimal conductance induced by a vesicle fusion was about 600pS which could be blocked by DIDS (if it was not blocked by DIDS later addition of mM concentration of $ZnCl_2$ eliminated the conductance). No conclusions could be drawn about the unit conductance of DIDS-sensitive and Zn^{++}-sensitive channels from single channel data.

8. No IP_3-gated Ca^{++} channel was found in the liver rough ER membrane.

9. No rynodine-sensitive Ca^{++} channel was found in the liver rough ER membrane.

10. No K^+ channel like the one present in SR membrane was found in the rough ER membrane.

BIBLIOGRAPHY

BIBLIOGRAPHY

1. Grant, A. and Burchell, A. (1990) *Biochem. Soc. Trans.,* **18**, 1251.

2. Meissner, G. and Allen, R. (1981) *J. Biol. Chem.,* **256**, 6413.

3. Somlyo, A. P.,Bond, M. and Somlyo, A.V. (1985) *Nature*, **314**, 622.

4. Jong, Yuh-Jiin, Sheldon, A., Zhang GuoH and Kraus Friedmann,N. (1990) *J. Membr. Biol.* **118**, 49.

5. Milner, R. E., Baksh, S., Shemanko, C., Carpenter, M. R., Smillie, L., Vance, J. E., Opas, M. and Michalak, M. (1991) *J. Biol. Chem.,* **266**, 7155

6. Rana, R. S. and Hokin L. E. (1990) *Physiol. Rev.*, **70**, 115.

7 Berridge, M. J. (1987) *Ann. Rev. Biochem.*, **56**, 159.

8 Berridge, M.J., Buchan, P. B. and Heslop, J. P. (1984) *Mol. Cell. Endocrinol.,* **36**, 37.

9 Dougherty, R. W., Godfrey, P. P., Hoyle, P. C., Putney, J. W. and Freer, R. J. (1984) *Biochem. J.*, **222**, 307.

10. Delfert, D. M., Hill, S., Pershadsingh, H. A., Sherman, W. R. and Mcdonald, J. M. (1986), *Biochem. J.*, **236**, 37.

11. Henne, V. and Soling, H-D. (1986) *FEBS Lett.*, **202**, 267.

12. Prentki, M., Wollheim, C.B. and Lew, P. D. (1984) *J. Biol. Chem.,* **259**, 13777.

13. Suematsu, E., Hirata, M., Sasaguri, T., Hashimoto, T. and Kuriyama, H. (1985) *Comp. Biochem. Physiol.*, **82A**, 645.

14. Brass, L. F. and Joseph, S. K. (1985) *J. Biol. Chem.*, **260**, 15172.

15. Smith, J. B., Smith, L. and Higgins B. L. (1985) *J. Biol. Chem.*, **260**, 14413.

16. Supattapone, S., Worley, P. F., Baraban, J. M. and Snyder, S. H. (1988) *J. Biol. Chem.*, **263**, 1530.

17. Maeda, N., Niinobe, M. and Mikoshiba, K. (1990) *EMBO J.*, **9**, 61.

18. Furuichi, T., Yoshikawa, S., Miyawaki, A., Wada, K., Maeda, N. and Mikoshiba, K. (1989) *Nature* ,**342**,32.

19. Ferris, C. D., Huganir, R. L., Supattapone, S. and Snyder S. H. (1989) *Nature* ,**342**, 87.

20. Ferris, C. D., Huganir, R. L. and Snyder, S. H. (1990) *Proc. Natl. Acad. Sci. USA*, **87**, 2147.

21. Hingorani, S., Ondrias, K., Agnew, W. and Ehrlich, B. E. (1990) *Soc. Neurosci. Abstr.*, **16**, 1018.

22. Maeda, N., Kawasaki, T., Nakade, S., Yokota, N., Taguchi, T., Kasai, M. and Mikoshiba, K. (1991) *J. Biol. Chem.*, **266**,1109.

23. Chadwick, C. C., Saito, A. and Fleischer, S. (1990) *Proc. Natl. Acad. Sci. USA* ,**87**, 2132.

24. Mignery, G. A. and Sudhof, T.C. (1990) *EMBO J.*, **9**. 3893.

25. Marks, A. R., Tempst, P., Chadwick, C. C., Riviere, L, Fleisher, S and Nadal-Ginard, B. (1990) *J. Biol. Chem.*, **265**, 20719.

26. Meyer, T., Wensel, T. and Stryer, L. (1989) *Biochemistry* ,**29**, 32.

27. Watras, J., Bezprozvanny, I. and Ehrlich, B. E. (1991) *J. Neurosci.*, **11**, 3239.

28. Nunn, D. L. and Taylor, C. W. (1990) *Biochem. J.*, **270**, 227.

29. Muallem, S., Schoeffield, Pandol, S. and Sachs G. (1985) *Proc. Natl. Acad. Sci. USA*, **82**, 4433.

30. Rossier, M. F., Bird, G. St. J. and Putney, J. W. (1991) *Biochem. J.*, **274**, 643.

31. Volpe, P., Krause, K-H, Hashimoto, S., Zorzato, F., Pozzan, T., Meldolesi, J. and Lew, D. P. (1988) *Proc. Natl. Acad. Sci.*, **85**, 1091.

32. Smith, J.S., Coronado, R. and Meissner, G. (1985) *Nature*, **316**, 446.

33. Smith, J. S., Coronado, R. and Meissner (1986) *J. Gen. Physiol.*, **88**, 573.

34. Vassilev, P. M., Kanazirska, M. P. and Tien, H. T. (1987) *Biochim. Biophys. Acta.*, **897**, 324.

35. Ashley, R. H. (1989) *J. Membr. Biol.*, **111**, 179.

36. Bezprozvanny, I., Watras, J. and Ehrlich, B. E. (1991) *Nature*, **351**, 751.

37. Ross. C. A., Meldolesi, J., Milner, T. A., Satoh, T., Supattapone, S. and Snyder, S. H. (1989) *Nature,* **339**, 468.

38. Ellisman, M. H., Deerinck, T. J., Ouyang, Y., Beck, C. F., Tanksley, S. J., Walton, P. D., Airey, J. A. and Sutko, J. L. (1990) *Neuron*, **5**, 135.

39. Shoshan-Barmatz, V. (1990) *FEBS Lett.*, **263**, 317.

40. Shoshan-Barmatz, V., Pressley, T. A., Higham, S. and Krauss-Friedmann, N. (1991) *Biochem. J.*, **276**, 41.

41. Simon, S. M., Blobel, G. and Zimmerberg J. (1989) *Proc. Natl. Acad. Sci. USA*, **86**, 6176.

42. Simon, S. M. and Blobel G. (1991) *Cell*, **65**, 371.

43. Blobel, G and Dobberstein, B. (1975) *J. Cell. Biol.*, **67**, 835.

44. Miller, C., Arvan, P., Telford, J. N. and Racker, E. (1976) *J. Membr. Biol.*, **30**, 271.

45. Cohen, F. S. (1986) in *Ion Channel Reconstitution*, Miller, C. (ed.), Plenum Publishing Corp., New York.,p. 131.

46. Cohen, F. S., Niles, W. D. and Akabas, M. H. (1989) *J. Gen. Physiol.*, **93**, 201.

47. Bormann, J., Hamill, O. P. and Sakmann, B. (1987) *J. Physiol. (Lond.)*, **385**, 243

48. Anderson, M. P., Gregory, R. J., Thompson, S., Souza, D. W., Paul, S., Mulligan, R. C., Smith, A. E. and Welsh, M. J. (1991) *Science* ,**253**, 202.

49. Tabcharani, J. A., Chang, Xiu-Bao, Riordan, J. R. and Hanrahan, J. W. (1992) *Biophys. J.*, **62**, 1.

50 Marty, A., Tan, Y. P. and Trautmann, A. (1984) *J. Physiol. (Lond.)*, **357**, 293.

51. Barish, M. E. (1983) *J. Physiol. (Lond.)*, **342**, 309.

52. Soejima, M. and Kokubun, S. (1988) *Pflugers Achiv.*, **411**, 304.

53. Pacaud, P, Loirand, G., Lavie, J. L., Mironneau, C. and Mironneau, J. (1989) *Pflugers. Archiv.*, **413**, 629.

54. Harvey, R. D., Clark, C. D. and Hume, J. R. (1990) *J. Gen. Physiol.*, **95**, 1077.

55. Gogelein, H. (1988) Biochim. *Biophys. Acta.*, **947**, 521.

56. Miller, C. and Richard, E. A. (1990) in *Chloride Channels and Carriers in Nerve, Muscle and Glial Cells*, Alvarez-Leefmans, F. J. and Russel, J. M. (eds.) , Plenum Press, New York and London, p. 383.

57. Gray, P. T. A., Beevan, S. and Ritchie, J. M. (1984) *Proc. R. Soc. (Lond.) [Biol.]*, **221**, 395.

58. Blatz, A. L. (1990) in *Cl^- Channels and Carriers in Nerve, Muscle and Glial cells*, Alvarez-Leefmans, F. J. and Russel, J. M. (eds.) , Plenum Press, New york and London, p.407.

59. Hanrahan, J. W., Alles, W. P. and Lewis, S. A. (1985) *Proc. Natl. Acad. Sci. USA*, **82**, 7791.

60. Woll, K. H., Leibowitz, M. D., Neumcke, B. and Hille, B. (1987) *Pflugers Archiv.*, **410**, 632.

61. Nelson, D. J., Tang, J. M. and Palmer, L. G. (1984) *J. Membr. Biol.*, **80**, 81.

62. Tanifuji, M., Sokabe, M. and Kasai, M. (1987) *J. Membr. Biol.*, **99**, 103.

63. Hals, G. D., Stein, P. G. and Palade, P. T. (1989) *J. Gen. Physiol.*, **93**, 385.

64. Colombini, M. (1986) in *Ion Channel Reconstitution*, Miller, C. (ed.), Plenum Press, New York and London, p.533.

65. Halm, D. R., Rechkemmer, G. R., Schoumaker, and Frizzel, R. A. (1988) *Am. J. Physiol.*, **254** (*Cell Physiol.* **23**), C505.

66. Frizzel, R. A., Halm, D. R., Rechkemmer, G. and Shoemaker, R. L. (1986) *Fed. Proc.*, **45**, 2727.

67. Jetten, A. M., Yankaskas, J. R., Stutts, M. J., Willumsen, N. J. and Boucher, R. C. (1989) *Science* ,**244**, 1472.

68. Chen, J. H., Schulman, H. and Gardner, P. (1989) *Science*, **243**, 657.

69. Franciolini, F. and Nonner, W. (1987) *J. Gen. Physiol.*, **90**, 453.

70. Lukacs, G. L. and Moczydlowski, E. (1990) *J. Gen. Physiol.*, **97**, 707.

71. Hamill, O., Marty, A., Neher, E., Sakmann, B. and Sigworth, F. J. (1981) *Pflugers Archiv.*, **391**, 85.

72. Miller, C. (ed.) (1986) *Ion Channel Reconstitution*, Plenum Press, New York and London.

73. Hanke, W. (1986) in *Ion Channel Reconstitution*, (Miller, C. ed.) Plenum Press, New York and London, p. 141.

74. Tank, D. W. and Miller, C. (1986) in *Single Channel Recording,* Sakmann, B. and Neher, E. (eds.), Plenum Press, New York and London, p91.

75. Suarez-Isla, B. A., Wan, K., Lindstrom, J. and Montal, M. (1983) *Biochemistry*, **22**, 2319.

76. Coronado, R. and Lattore, R. (1983) *Biophys. J.*, **43**, 231.

77. Dallner, G. (1974) in *Methods in Enzymology*, Vol. **31**, Fleischer, S. and Packer, L. (eds.), Academic Press, New York, p. 191.

78. Rothschild, J. (1963) *Biochem. Soc. Symp.*, **22**, 4.

79. Lowry. O. H., Rosebrough, N. J., Farr, A. L. and Randall, R. J. (1951) *J. Biol. Chem.*, **193**, 265.

80. Fleischer, S. and Fleischer, B. (1967) in *Methods in Enzymology*, Vol. **10**, Estabrook, R. W. and Pullman, M. E. (eds.), Academic Press, New York, p. 406.

81. Akabas, M. H., Cohen, F. S. and Finkelstein, A. (1984) *J. Cell. Biol.*, **98**, 1063.

82. Young, T. M. and Young, J. D. (1984) *Biochim. Biophys. Acta.*, **775**, 441.

83. Woodbury, D. J. and Miller, C. (1990) *Biophys. J.*, **58**, 833.

84. Niles, W. D. and Cohen, F. S. (1987) *J. Gen. Physiol.*, **90**, 703.

85. Schenkman, J. B. and Cinti, D. L. (1978) in *Methods in Enzymology*, Vol. **52**, Fleischer, S. and Packer, L. (eds.), Academic Press, New York, p. 83.

86. Tien, H. T. (1974) *Bilayer Lipid Membrane (BLM) : Theory and Practice*, Marcel Dekker, New York.

87. Hille, B. (1984) *Ionic Channels of Excitable Membranes*, Sunderland, MA: Sinauer.

88. Gram, T. E. (1974) in *Methods in Enzymology*, Vol. **31**, Fleischer, S. and Packer, L. (eds.), Academic Press, New York, p. 225.

89. Cinti, D. L., Moldeus, P. and Schenkman J. B. (1972) *Biochem. Pharmacol.*, **21**, 3249.

90. Fabiato, A. (1988) in *Methods in Enzymology*, Vol. **157**, Fleischer, S. and Fleischer, B. (eds.), Academic Press, New York, p. 378.

91. Robinson, R. A. and Stokes, R. H. (1959) *Electrolyte Solutions*, Butterworth & Co., Ltd., London.

92. Eisenman, G. and Horn, R. (1983) *J. Membr. Biol.*, **76**, 197.

93. Inoue, I. (1985) *J. Gen. Physiol.*, **85**, 519.

94. Gray, P. T. A. and Ritchie, J. M. (1986) *Proc. R. Soc. Lond.*, **B. 228**, 267.

95 Bosma, M. M. (1986) *Biophys. J.*, **49**, 413a.

96. Hutter, O. F. and Warner, A. E. (1967) *J. Physiol. (Lond.)*, **189**, 445.

97. Spalding, B. C., Swift, J. G., Gefell, D. J. and Horowicz, P. (1986) *Biophys. J.*, **49**, 218a.

98. Woodbury, J. W. and Miles, P. R. (1973) *J. Gen. Physiol.*, **62**, 324.

99. Stanfield, P. R. (1973) *J. Physiol. (Lond.)*, **209**, 213.

100. Kometani, T. and Kasai, M.(1980) *J. Membr. Biol.*, **41**, 295.